V. THEORETICAL PHYSICS

OVERVIEW

Our research addresses important problems in theoretical nuclear physics involving the structure and dynamics of hadrons and nuclei. There is strong emphasis on comparison with data from Argonne's ATLAS facility, from JLab, and from other laboratories around the world, and predicting phenomena observable with a rare isotope accelerator. Our work includes the modeling and application of quantum chromodynamics (QCD) to light- and heavy-hadron structure at zero temperature and density, and at the extremes of temperature and density appropriate to the early universe, neutron stars, and RHIC experiments. We develop reaction theories to use in exploring hadron structure using the data from meson and nucleon-resonance production experiments at JLab, MIT-Bates and Mainz. We construct realistic two- and three-nucleon potentials that give accurate fits to nucleon-nucleon elastic scattering data and properties of light nuclei, and use them in detailed many-body calculations of light and near closed-shell nuclei, nuclear matter and neutron stars, and in a variety of astrophysically important electroweak reactions. Our nuclear structure and reaction studies include coupled-channels calculations of heavy-ion reactions near the Coulomb barrier, and calculations of observables in breakup reactions of nuclei far from stability. We also study high-spin deformation and the structure of the heaviest elements at the mean-field level, and work toward an understanding of the interplay between collective modes at the many-body level. Additional research is pursued in atomic physics, neutron physics, quantum computing, and fundamental quantum mechanics. Several of our projects involve major numerical simulations using the massively parallel computer systems at Argonne and NERSC.

A. NUCLEAR DYNAMICS WITH SUBNUCLEONIC DEGREES OF FREEDOM

The objective of this research program is to investigate the role of: quark-gluon degrees of freedom in hadron structure and interactions, and in nuclear dynamics; the development and application of reaction theories for use in exploring hadron structure using the data from meson and nucleon-resonance production experiments at modern experimental facilities; and to investigate relations of Poincaré covariant dynamics specified by mass operators to complementary dynamics specified by Green functions.

At the level of quark-gluon degrees of freedom, the Dyson-Schwinger equations (DSEs) provide a Poincaré covariant, nonperturbative method for studying QCD in the continuum. The existence of symmetry preserving truncations enables the simultaneous exploration of phenomena such as: confinement, dynamical chiral symmetry breaking, and bound state structure and interactions. In addition the DSEs provide a generating tool for perturbation theory and hence yield model-independent results for the ultraviolet behavior of strong interaction observables. This means that model studies facilitate the use of physical processes to constrain the long-range behavior of the quark-quark interaction in QCD, which is poorly understood and whose elucidation is a key goal of modern experimental programs. The last year saw numerous successful applications. For example, we showed that a Ward-Takahashi identity preserving Bethe-Salpeter kernel can always be calculated explicitly from a dressed-quark-gluon vertex whose diagrammatic content is enumerable and that this kernel is nonplanar in all but the simplest case. In doing so we made clear that this simplest case, the rainbow-ladder truncation, is the first term in a systematic and nonperturbative scheme, and thereby explained its quantitative success. Moreover, in a direct application of nonequilibrium quantum mean field theory we demonstrated that a 9-TW-peak x-ray free electron laser could produce a plasma of electron-positron pairs directly from the QED vacuum.

At the level of meson and baryon degrees of freedom, we are continuing our effort to develop dynamical models for interpreting the data of few-GeV hadron reactions in terms of the quark-gluon substructure of nucleon resonances (N^*) as predicted by various QCD-based hadron models. In the past year we have extended our dynamical model for pion electroproduction in the Δ region to also investigate neutrino induced reactions. It is found that the axial N-Δ transitions also contain large pion cloud contributions and the existing neutrino induced pion production data are consistent with the constituent quark model. For investigating higher mass N^* resonances, we developed a unitary coupled-channel $\pi\pi N$ model. In our investigation of vector meson photoproduction, we showed that coupled-channel effects are essential in identifying the nucleon resonances using spin observables. Finally, we investigated the quark-exchange mechanisms of deuteron photodisintegration at 2-6 GeV, with the aim of exploring the transition from a hadronic picture to a quark-gluon picture of nuclear dynamics.

Relativistic quantum dynamics requires a unitary representation of space-time symmetries (Poincaré group) and localization of states, such that states localized in relatively space-like regions are causally independent. Recent mathematical developments indicate how manifolds of localized states can be defined strictly within the framework of relativistic quantum mechanics without reference to infinite systems.

a.1. Quantum Effects with an X-ray Free Electron Laser (C. D. Roberts, S. M. Schmidt,* and D.V. Vinnik†)

A quantum kinetic equation coupled with Maxwell's equation was used to estimate the laser power required at an X-ray free-electron laser (XFEL) facility to expose intrinsically quantum effects in the process of QED vacuum decay via spontaneous pair production. We found that a 9-TW-peak XFEL laser with photon energy of 8.3 keV could be sufficient to initiate particle accumulation and the consequent formation of a plasma of spontaneously produced pairs (Fig. V-1). In that plasma, the evolution of the particle number will exhibit non-Markovian aspects of the strong-field pair production process, and the internal currents will generate an electric field whose interference with that of the laser leads to plasma oscillations. An article describing this work was published.[1]

[1]C. D. Roberts, S. M. Schmidt and D. V. Vinnik, Phys. Rev. Lett. **89**, 153901 (2002).
*University of Tuebingen, Germany, †Helmholtz-Gemeinschaft, Germany.

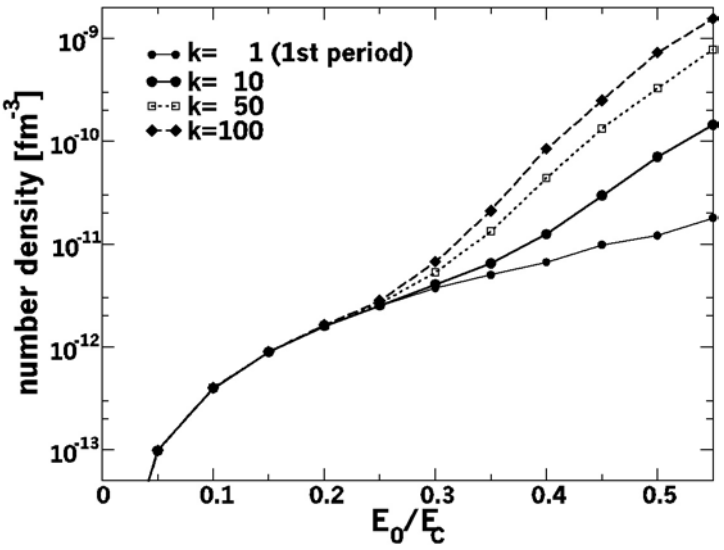

Fig. V-1. Peak particle number density in the laser spot volume versus laser field strength, measured in terms of the critical field: $eE_{cr} = mc^2$. (k counts the number of elapsed laser periods.) There is a striking qualitative change at $E_0 \approx 0.25\ E_{cr}$, which marks the onset of particle accumulation; viz., beyond this point the number of particles in the spot volume increases materially over the lifetime of the lasing pulse.

a.2. Nucleon Mass and Pion Loops (M. B. Hecht, C. D. Roberts, M. Oettel,* A. W. Thomas,* S. M. Schmidt,† and P. C. Tandy‡)

We solved Poincaré covariant Faddeev equations for the nucleon and delta to illustrate that an internally consistent description in terms of confined-quark and non-pointlike confined-diquark-correlations can readily be obtained. Subsequently, we calculated the πN-loop induced self-energy corrections to the nucleon's mass and showed them to be independent of whether a pseudoscalar or pseudovector coupling is used. Applying phenomenological constraints, we argued that this self-energy correction reduces the nucleon's mass by up to several hundred MeV. However, we demonstrated that this effect does not qualitatively alter the picture, suggested by the Faddeev equation, that baryons are quark-diquark composites, although neglecting the π-loops leads to a quantitative overestimate of the nucleon's axial-vector diquark component. An article describing this work was published.[1]

*CSSM, University of Adelaide, Australia, †University of Tübingen, Germany, ‡Kent State University.
[1]M. B. Hecht, C. D. Roberts, S. M. Schmidt, P. C. Tandy and A. W. Thomas, Phys. Rev. C **65**, 055204 (2002).

a.3. Bethe-Salpeter Equation and a Nonperturbative Quark-Gluon Vertex

(C. D. Roberts, A. Bender,* W. Detmold,* and A. W. Thomas*)

A Ward-Takahashi identity preserving Bethe-Salpeter kernel can always be calculated explicitly from a dressed-quark-gluon vertex whose diagrammatic content is enumerable. We illustrated that fact using a vertex obtained via the complete resummation of dressed-gluon ladders. While this vertex is planar, the vertex-consistent kernel is nonplanar and that is true for any dressed vertex. In an exemplifying model, the rainbow-ladder truncation of the gap and Bethe-Salpeter equations yielded many results; e.g., π- and ρ-meson masses, that are changed little by including higher-order corrections. Moreover, we saw that the bulk of the ρ-π mass splitting is present in the chiral limit and that its value is not materially influenced by improving the kernel. These results demonstrate that the mass difference is driven by the DCSB mechanism and is not the result of a carefully contrived chromo-hyperfine interaction. In addition, it was apparent that repulsion generated by nonplanar diagrams in the vertex-consistent Bethe-Salpeter kernel for quark-quark scattering is sufficient to guarantee that diquark bound-states do not exist. This analysis confirms the importance of preserving symmetries in studies of QCD's bound states. An article describing this work was published.[1]

*CSSM, University of Adelaide, Australia.

[1]A. Bender, W. Detmold, C.D. Roberts and A.W. Thomas, Phys. Rev. C **65** (2002) 065203.

a.4. Dyson-Schwinger Equations: A Tool for Hadron Physics

(C. D. Roberts and P. Maris*)

Dyson-Schwinger equations furnish a Poincaré covariant framework within which to study hadrons. However, their application has long been plagued by concerns over the need to employ a truncation scheme in order to arrive at a tractable problem. It was recently shown that there exists at least one systematic, nonperturbative, symmetry-preserving DSE truncation procedure; and this has enabled the proof of exact, model-independent results. For example, the gap equation reveals that dynamical chiral symmetry breaking is tied to the long-range behavior of the strong interaction, which is thereby constrained by observables, and the pion is precisely understood, and seen to exist simultaneously as a Goldstone mode and a bound state of strongly dressed quarks. The rainbow-ladder truncation is the leading-order term in the systematic scheme. That realization has enabled the systematic error associated with this simplest truncation to be quantified, and that explains and underpins a one-parameter model efficacious in describing an extensive body of mesonic phenomena. Incipient applications to baryons have brought successes and encountered challenges familiar from early studies of mesons, and promise a covariant field theory upon which to base an understanding of contemporary large momentum transfer data. This body of work reveals that the momentum-dependent *dressing* of the propagators of QCD's elementary excitations is a fundamental feature of strong QCD that is observable in hadron physics. We completed an extensive review, explaining these foundations and reviewing many applications, which was accepted for publication.

*North Carolina State University.

a.5. Facets of Confinement and Dynamical Chiral Symmetry Breaking
(C. D. Roberts, P. Maris,* A. Raya,† and S. M. Schmidt‡)

The gap equation is a cornerstone in understanding dynamical chiral symmetry breaking and, perhaps, confinement too. The existence of a symmetry-preserving truncation enables proofs of important results and also a gap-equation-based analysis of contemporary lattice data on quark and gluon propagators. The available lattice data is for quenched QCD and this exploratory study suggests that physical observables are materially underestimated in the quenched theory: the pion decay constant by as much as a factor of two. In addition it re-emphasizes that multiplicative renormalizability can provide very useful constraints on the gap equation's kernel. An article describing this research was submitted for publication.

*North Carolina State University, †Universidad Michoacana de San Nicolás de Hidalgo, Mexico, ‡Helmholtz-Gemeinschaft, Germany.

a.6. Concerning the Quark Condensate (C. D. Roberts, K. Langfeld,* R. Pullirsch,† H. Markum,† and S. M. Schmidt‡)

We verified that the gauge-invariant trace of the massive dressed-quark propagator possesses a spectral representation, with a non-negative spectral density $\rho(\lambda)$, when considered as a function of the current-quark mass. This is key to establishing that the OPE condensate, which sets the ultraviolet scale for the momentum-dependence of the trace of the dressed-quark propagator, does indeed measure the density of far-infrared eigenvalues of the gauge-averaged massless Dirac operator, à la the Banks-Casher relation. This relation is intuitively appealing because a measurable accumulation of eigenvalues of the massless Dirac operator at zero-virtuality expresses a mass gap in its spectrum. In our continuum analysis we found that one requires $am \leq (a\Lambda_{QCD})^3$ if $\rho(\lambda) = 0$ is to provide a veracious estimate of the OPE condensate. The residue at the lowest-mass pole in the flavor-nonsinglet pseudoscalar vacuum polarization provides a measure of the OPE condensate that is accurate for larger current-quark masses. An article describing this work was accepted for publication.

*University of Tübingen, Germany, †Technical University of Vienna, Austria, ‡Helmholtz-Gemeinschaft, Germany.

a.7. Analysis of a Quenched Lattice-QCD Dressed-Quark Propagator
(C. D. Roberts, M. S. Bhagwat,* M. A. Pichowsky,* and P. C. Tandy*)

We studied quenched-QCD using a rainbow-ladder truncation of the Dyson-Schwinger equations and demonstrated that existing results from lattice simulations for the dressed-gluon and –quark Schwinger functions can be correlated via a gap equation. As usual, the ultraviolet behavior of this equation's effective interaction is fully determined by perturbative QCD. For the infrared, we employed a simple Ansatz whose parameters were fixed in a least squares fit of the gap equation's solutions to lattice data on the dressed-quark mass function at available current-quark masses. With our best-fit parameters the mass functions obtained from the gap equation were indistinguishable from the lattice results (Fig. V-2). To correlate the lattice's dressed-gluon and dressed-quark Schwinger functions it was necessary for the kernel to exhibit infrared enhancement over and above that observed in the dressed-gluon function alone. In our model we ascribed that to an enhancement of the quark-gluon vertex. The gap equation provides a solution for the dressed-quark Schwinger function at arbitrarily small current-quark masses and, in particular, in the chiral limit: no extrapolation is involved. It may therefore be used as a tool with which to estimate the chiral limit behavior of the lattice propagator. In addition, knowing the gap equation's kernel, it is straightforward to construct symmetry-preserving Bethe-Salpeter equations whose bound state solutions describe mesons. This enabled an analysis which indicates that chiral and physical pion observables are significantly smaller in the quenched theory than in full QCD. An article describing this work was submitted for publication.

*Kent State University.

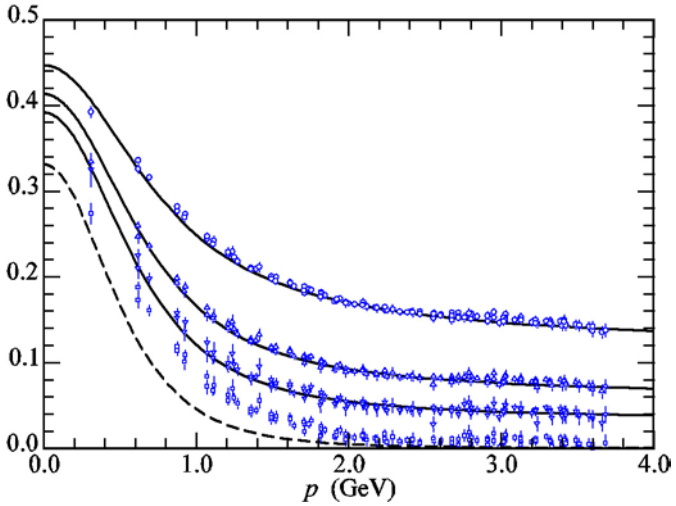

Fig. V-2. Data, upper three sets, lattice results for the quark mass function (in GeV); lower points (circles), linear extrapolation of lattice results to the chiral limit; i.e., am = 0. Solid curves, our best-fit-interaction gap equation solutions for the mass function; dashed-curve, solution of the gap equation obtained in the chiral limit. There is a marked discrepancy between our chiral limit result, which is calculated directly, and the linear extrapolation of lattice data.

a.8. Comparison of Point-Form Quantum Mechanics and Quantum Field Theory (F. Coester, A. Krassnigg, and C. D. Roberts)

We will explore the extent to which a relationship exists between bound state studies in relativistic quantum field theory and in relativistic quantum mechanics. Dyson-Schwinger equations provide a Poincaré covariant framework for continuum bound state studies in quantum field theory. In relativistic quantum mechanics, we adopt the point form because it, too, is manifestly covariant. In quantum mechanics one studies a mass operator and its eigenvalues. A key question is whether a mass operator and Hilbert space exist that can describe features equivalent to those obtained in quantum field theory. To be concrete, we will first compare results obtained for vector mesons in the two approaches, seeking to identify elements of qualitative equivalence and differences that may indicate model-dependent artifacts. An extension to axial-vector mesons will follow. These states are particularly sensitive to long-range features of QCD's interaction; viz., aspects of confinement. A study of pion properties is expected to be crucial. The dichotomous nature of the pion, as both a Goldstone mode and bound state of massive constituents, is likely to make a valid description in quantum mechanics impossible.

a.9. Axial-Vector Diquarks in the Baryon (A. Krassnigg and C. D. Roberts)

It was shown that a product Ansatz for the nucleon's Faddeev amplitude using only a scalar-diquark can provide a good description of leptonic and nonleptonic couplings and form factors, with some notable exceptions; e.g., the neutron's charge radius and axial vector coupling. Properly incorporating the lower component of the nucleon's spinor helps somewhat in addressing these exceptions. However, discrepancies remain, and we anticipate that their amelioration requires the inclusion of axial-vector diquark correlations and a pion cloud. We plan to explore this, and quantify the effects of these contributions on $G^p_E(q^2)/G^p_M(q^2)$ and the $N \rightarrow \Delta$ transition form factor, current data on both of which we believe are dominated by nonperturbative dynamics.

a.10. Valence-Quark Distributions in the Nucleon (A. Krassnigg and C. D. Roberts)

The pion provides the simplest theoretical subject for a calculation of the valence quark distribution function. However, pion targets are not readily available for experiment and the most reliable measurements of quark distribution functions were performed on nucleon targets. We intend to extend the approach developed for the pion so as to employ it in a calculation of the nucleon's valence quark distribution. In the first studies, the target nucleon will be represented by a quark-plus-scalar-diquark product Ansatz for its Faddeev amplitude. This promises to provide the first Poincaré covariant calculation of the nucleon's valence quark distribution function. Improving the nucleon model via the inclusion of axial-vector diquark correlations and a pion cloud will enable the drawing of a connection between deep inelastic scattering measurements and the "soft physics" wrapped up in nucleon structure. For example, it will provide a means of testing the validity and importance of diquark clustering in the nucleon, and the relation between the *d/u*-ratio at large-*x* and confinement, as it is exhibited in the momentum-space extent of the Faddeev amplitude.

a.11. J/ψ Suppression as a Signal of Quark Gluon Plasma Formation (C. D. Roberts, D. B. Blaschke,* and Yu. L. Kalinovsky†)

We developed a successful approach to describing heavy-meson observables at zero temperature. That enables a reliable extrapolation into the domain of nonzero temperature, which is relevant to the RHIC program. The suppression of the J/ψ production cross section is touted as a unique signal of quark gluon plasma formation, and such suppression was observed at CERN. We propose to study J/ψ production in the expectation that additional insight will follow from the Dyson-Schwinger equations' capacity to unify nonperturbative aspects of light- and heavy-meson observables via a microscopic description using QCD's elementary excitations. Our initial focus is the T-dependence of J/ψ break-up by hadronic comovers; *i.e.,* the substructure induced T-dependence of those interactions with other mesons in the medium that dissociates the J/ψ. These processes are likely to be affected by the dramatic T-dependence of the dressed-light-quark mass function in the neighborhood of the QGP phase boundary and a possible T-dependent reduction in the mass of the open-charm final states. Our goal is to elucidate the mechanisms involved and the fidelity of J/ψ suppression as a signal of quark gluon plasma formation.

*University of Rostock, Germany, †LCTA, JINR, Dubna, Russia.

a.12. Particle Ratios at RHIC and Chemical Freeze-Out (S. Schramm, D. Zschiesche,* H. Stöcker,* and J. Schaffner-Bielich†)

We investigated hadronic particle production in ultrarelativistic heavy-ion collisions at RHIC. Thermodynamical equilibrium calculations of particle production in high energy particle- and nuclear collisions have been carried out for a long time. Experimental data for hadron abundances and ratios have been obtained in heavy-ion collisions at the SIS, AGS, SPS and more recently at the RHIC facility.

The plethora of data revived interest in extracting a common temperature and chemical potential for the chemical freeze-out point that determines the particle ratios using a thermal equilibrium model analysis. The experimentally determined hadron ratios can be fitted quite well with simple non-interacting gas models, if a sudden breakup of a thermalized source is assumed and the subsequent feeding of the various channels from strongly decaying higher resonances is taken into account. From the χ^2 freeze-out fits one has constructed a quite narrow band of freeze-out values in the T-μ_B plane. The extracted freeze-out parameters are close to the assumed phase transition curve for SPS and RHIC energies. However, if the system passes through the vicinity of the phase transition (or through the crossover range) as suggested by the data for T and μ_B, one cannot neglect the very in-medium effects that are responsible for the phase transition in the first place. Thus, non-interacting gas models, as they completely neglect any kind of possible in-medium modification, can only yield limited insight. Therefore, we based our studies on a relativistic self-consistent hadronic 3-flavor model. One can view the model as a thermodynamically consistent effective theory or as a toy model that includes the restoration of chiral symmetry at high temperatures or densities. In either case the model incorporates temperature and density dependent hadronic masses and effective chemical potentials.

Depending on the chosen parameters and degrees of freedom, different scenarios for the chiral phase change are predicted by the model: strong or weak first order phase transition or a crossover. The transitions take place around T_c = 155 MeV, in qualitative agreement with lattice predictions for the critical temperature for the onset of a deconfined and chirally restored phase.

A whole range of particle ratios are calculated in the SU(3) model and compared with the RHIC data for Au + Au at √130 AGeV. In addition a comparison with non-interacting gas calculations was performed.

Since different parameterizations of the model show qualitatively different phase transition scenarios, we investigate whether the particle production, *i.e.* the chemistry of the system, is sensitive to the phase transition behavior. Since we have shown that the current data are described by all three different phase transition scenarios (strong first order, weak first order or smooth crossover) and the ideal gas model, we can so far neither favor nor rule out any one scenario. (See Fig. V-3).

In all interacting models the effective masses at freeze-out are shifted by up to 15% from their vacuum values. The fit values for the chemical freeze-out temperature and chemical potential depend on the order of the phase transition. The crossover case yields temperatures that are shifted by 15 MeV as compared to the non-interacting gas model while the model calculations with a first order phase transition show more than 30 MeV lower temperatures.

Strikingly, the fitted freeze-out points are located very close to the phase transition boundary in the first-order phase transition scenarios, but T is always smaller than T_c. This suggests that at RHIC the system emerges after passing through the chiral phase transition. This of course is only true if a first order phase transition does actually occur in QCD at small chemical potentials and high T. Furthermore, from our studies it becomes clear that a "freezing" of the relative abundances of various hadrons in the symmetric phase (at $T > T_c$) is definitely excluded.

*University of Frankfurt, †Brookhaven National Laboratory.

[1]D. Zschiesche, S. Schramm, J. Schaffner-Bielich, H. Stöcker, and W. Greiner, Phys.Lett. **B547**, 7 (2002).

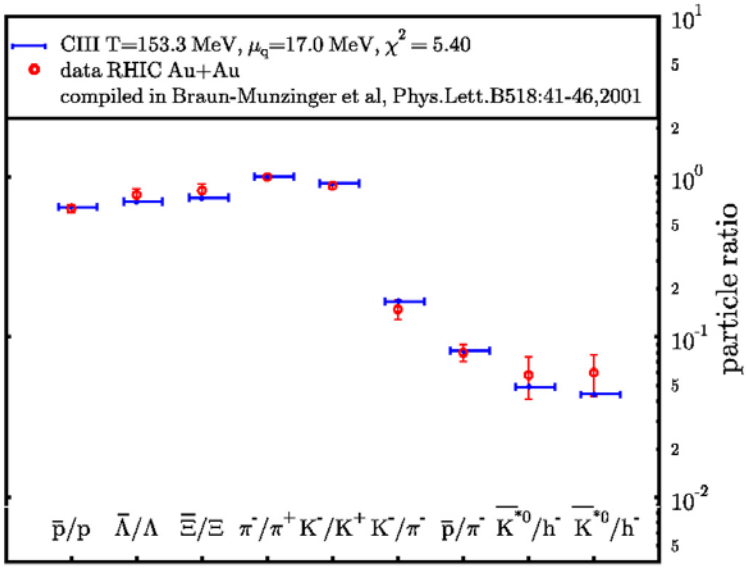

Fig. V-3. Hadronic particle ratios calculated with two different parameterizations[1] compared to experimental data obtained at RHIC.

a.13. HBT Analysis of Relativistic Heavy Ion Collisions (S. Schramm, D. Zschiesche,* and H. Stöcker*)

Bose-Einstein correlations in multi-particle production processes can provide important information on the space-time dynamics of fundamental interactions. Therefore correlations of identical pions produced in high-energy collisions of heavy ions could yield some insight into the characteristics of a hypothetical phase transition that might occur during the highly excited stage of the heavy-ion collision.

In particular, a potential first-order phase transition leads to a prolonged time of hadronization as compared to a smooth cross-over or a hadron gas with no symmetry restoration at all, and accordingly such a phase transition has been related to large Hanbury-Brown-Twiss (HBT) radii deduced from the 2-pion correlations. A coexistence phase of hadrons and quark gluon plasma droplets reduces the "explosivity" of the high-density matter before hadronization, prolonging the emission duration of pions.

The correlations should then depend on the hadronization, the critical temperature T_c and the latent heat of the transition. Calculations assuming a first-order phase transition are usually performed with an equation of state that is constructed by matching the bag model with an ideal hadron gas model, for which the latent heat of the transition is large. Consequently, also the predicted HBT radii are large. We studied the impact of a weaker first-order transition with relatively small latent heat and considered its influence on the space-time characteristics of the expansion and on HBT radii. As a limiting case we calculated the dynamics of the system for a smooth crossover transition at high temperatures.

Similar scenarios were investigated before, but without explicit reference to chiral symmetry restoration and dynamically changing hadron masses. To investigate the space-time dynamics and the influences of different types of phase transitions we performed a hydrodynamic simulation using various equations-of-state obtained from a chiral model. The hydrodynamical equations describe the collective evolution of the system, while the chiral model supplies the underlying equation of state. As the hot and dense central region of the heavy-ion collision expands in the longitudinal and transverse directions, the effective hadron masses approach their vacuum values. The initial excitation energy of the system is converted into collective flow and massive hadrons.

By considering various equations of state in the simulation one can get more information on how to discriminate between the different phase transition scenarios from observable correlations. The model used in this calculation contains only hadronic degrees of freedom, which limits the investigation to the chiral phase transition but not the deconfinement phase transition to a state of quarks and gluons. Still, the main effect as far as the collective expansion of the system is concerned originates from the difference in the latent heat for the transition, irrespective of its specific microscopic origin.

Within this approach we determined the HBT-radii relevant to experiments at CERN and RHIC and compared the results to NA49- and STAR data, respectively. One can clearly observe that a small latent heat, meaning a weak first-order phase transition or even a smooth cross over, leads to distinctly large radii in the HBT analysis for the side-direction R_{side} (signaling a rapid evolution of the system during the transition from light hadrons or quarks to the chirally broken phase and to small radii in out-direction R_{out}), which are closest to the data in almost all cases. (See Fig.V-4).

However, a quantitative description of the data, both at SPS energy as well as at RHIC energy, is not reached within the present hydrodynamical approach using the various SU(3) chiral EoS.

It was argued that the decay of a droplet of chirally symmetric matter from a region of negative pressure may yield small HBT radii, as well as a smaller ratio R_{out}/R_{side}. We are currently investigating this possibility.

More realistic freeze-out descriptions may improve the results. However, it appears probable that a quasi-adiabatic first-order phase transition with large latent heat, for which a hydrodynamical description should be adequate, cannot describe the pion HBT data from either SPS or RHIC experiments.

*University of Frankfurt.

[1]D. Zschiesche, S. Schramm, H. Stöcker, W. Greiner, Phys.Rev. C **65**, 064902 (2002).

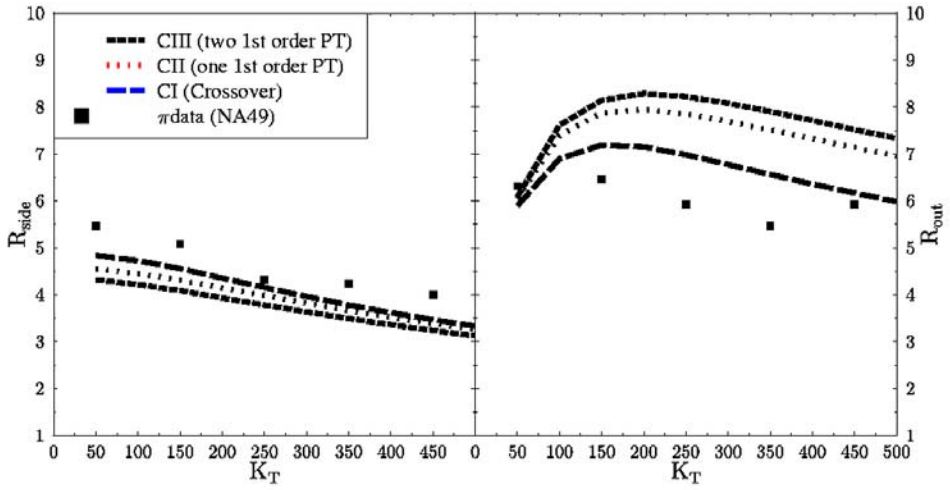

Fig. V-4. The figure shows the resulting HBT radii in the side-direction R_{side} and in the out-direction R_{out} relative to the scattering plane for central Pb + Pb collisions at SPS energy compared to data from the NA49 collaboration.[1] The general result suggests a better fit to the data assuming weak phase transitions.

a.14. Dyson Approach to Nonequilibrium Field Theory (B. Mihaila, F. Cooper,* and J. F. Dawson†)

Classical field theory: We study the domain of validity of a Schwinger-Dyson approach to non-equilibrium dynamics when $\langle\phi(x)\rangle \neq 0$. We perform exact numerical simulations of the one- and two-point functions of a single component $\lambda\phi^4$ field theory in 1 + 1 dimensions in the classical field theory case.[1] We compare these results to two self-consistent truncations of the Schwinger-Dyson equations which ignore three-point vertex function corrections. The first approximation, which we called the bare vertex approximation (BVA), sets the three-point function to one. It gives a promising description for $\langle\phi(x)\rangle \neq \phi(t)$. The second approximation, which ignores higher in 1/N corrections to the two-particle irreducible (2PI) generating functional is not as accurate for $\phi(t)$ for the case N = 1. Both approximations have serious deficiencies in describing the two-point function when $\phi(0) \gtrsim 0.4$.

Quantum field theory: We perform a detailed numerical investigation of the dynamics of a single component "explicitly broken symmetry" $\lambda\phi^4$ field theory in 1 + 1 dimensions,[2] using a Schwinger-Dyson equation truncation scheme based on ignoring vertex corrections (BVA). We assume here that the initial state is described by a Gaussian density matrix peaked around some non-zero value of $\langle\phi(0)\rangle$, and characterized by a single-particle Bose-Einstein distribution function at a given temperature. We compute the evolution of the system using three different approximations: Hartree, BVA and a related 2PI-1/N expansion, as a function of coupling strength and initial temperature. In the Hartree approximation, the static phase diagram shows that there is a first-order phase transition for this system. As we change the initial starting temperature of the system, we find that the BVA relaxes to a new final temperature and exhibits behavior consistent with a second-order phase transition. We find that the average fields equilibrate for arbitrary initial conditions in the BVA, unlike the behavior exhibited by the Hartree approximation, and we illustrate how $\langle\phi(t)\rangle$ and $\langle\chi(t)\rangle$ depend on the initial temperature and on the coupling constant. The Fourier transform of the two-point functions at late times can be fit by a Bose-Einstein distribution function whose temperature is independent of momentum. We interpret this as evidence for thermalization.

*Los Alamos National Laboratory, †University of New Hampshire.

[1]F. Cooper, J. Dawson, and B. Mihaila, Phys. Rev. D **67**, 51901(R) (2003).
[2]F. Cooper, J. Dawson, and B. Mihaila, Phys. Rev. D **67**, 56003 (2003.

a.15. Continuum Versus Periodic Lattice Monte Carlo Approach to Classical Field Theory (B. Mihaila and J. F. Dawson*)

We discuss two Monte Carlo approaches of obtaining the dynamical evolution of a classical ϕ^4 field theory system,[1] one based on a standard periodic lattice formulation in coordinate space, the other in momentum space. Both methods require the assumption of periodic boundary conditions, but the different levels at which this assumption is made allows the momentum-space approach to avoid certain artifacts of the lattice-based method. In particular, the intrinsic mismatch in initial conditions at finite cutoff values, results in different values of the "thermalized" field, at large times. The discrepancy is worse for smaller values of the cutoff, but the two approaches converge to the same result in the continuum limit. The mismatch in initial conditions is due to the fact that by using a finite-difference approximation for the spatial derivative operator together with the assumption of periodic boundary conditions on the lattice, we have, in fact introduced an approximation of the dispersion relation, which is now viewed as an expansion in the lattice spacing a. In order to improve the quality of the spatial derivative approximation in the lattice case, one would normally have to take the limit when the lattice spacing a goes to zero. We are, however, prevented from doing that, since the choice of the momentum cutoff Λ also determines the choice of the lattice spacing $a = \pi/\Lambda$. Consequently, we cannot improve the agreement of the lattice dispersion relation with the continuum for a given momentum-space cutoff. The momentum-space approach does not exhibit this limitation.

*University of New Hampshire.

[1]B. Mihaila and J. Dawson, Phys. Rev. D **65**, 71501(R) (2002).

a.16. Parallel Algorithm with Spectral Convergence for Nonlinear Integro-Differential Equations (B. Mihaila and R. E. Shaw*)

We discuss a numerical algorithm[1] for solving nonlinear integro-differential equations, and illustrate our findings for the particular case of Volterra type equations. The algorithm combines a perturbation approach meant to render a linearized version of the problem and a spectral method where unknown functions are expanded in terms of Chebyshev polynomials (El-gendi's method). From a computational point of view, each iteration involves two stages, namely initializing the relevant matrices and solving a linear system of equations. Both stages can be rendered parallel in a suitable manner, and the efficiency of the code increases when applied to complicated multi-step, multi-dimensional problems. This approach is shown to be suitable for the calculation of two-point Green functions required in next-to-leading-order studies of time-dependent quantum field theory.

*University of New Brunswick, Canada.

[1]B. Mihaila and R. E. Shaw, J. Phys. A: Math. Gen. **35**, 5315 (2002).

a.17. Dynamical Model of Weak Pion Production Reactions (T.-S. H. Lee, Toru Sato,* and D. Uno*)

The dynamical model of pion electroproduction developed in an Argonne-Osaka University collaboration[1] has been extended to investigate the weak pion production reactions. With the Conserved Vector Current (CVC) hypothesis, the weak vector currents are constructed from electromagnetic currents by isospin rotations. Guided by the effective chiral Lagrangian method and using the unitary transformation method developed previously, the weak axial vector currents for π production are constructed with no adjustable parameters. In particular, the N-Δ transitions at $Q^2 = 0$ are calculated from the constituent quark model and their Q^2-dependence is assumed to be identical to that determined in the study of pion electroproduction. The main feature of our approach is to renormalize these bare N-Δ form factors with the dynamical pion cloud effects originating from the non-resonant π production mechanisms. The predicted cross sections of neutrino-induced pion production reactions, $N(\nu_\mu,\mu^-\pi)N$, are in good agreement with the existing data. This is illustrated in Figs.V-5a and V-5b. We show that the renormalized (dressed) axial N-Δ

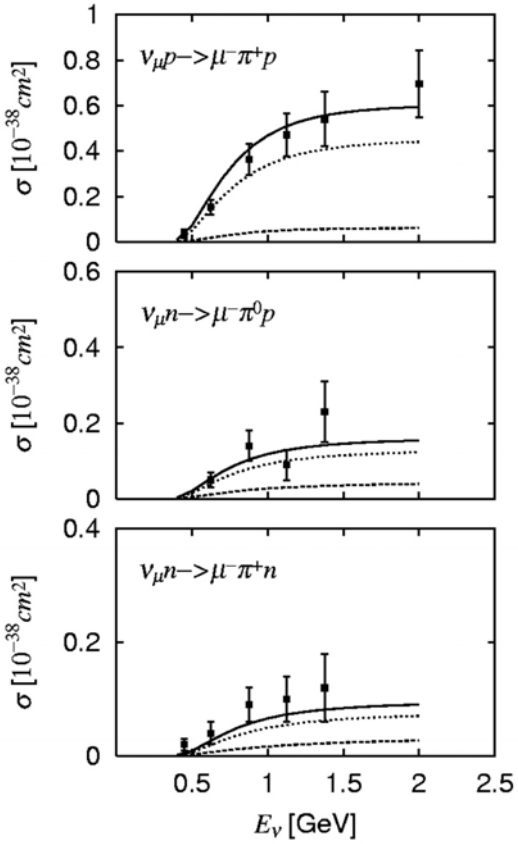

Fig. V-5a. Total cross sections of $N(\nu,\mu^-\pi^+)N$ reactions. The solid curves are from full calculations. The dashed curves are from turning off pion cloud effects on N-Δ transitions. The dotted curves are the contributions from the non-resonant amplitude.

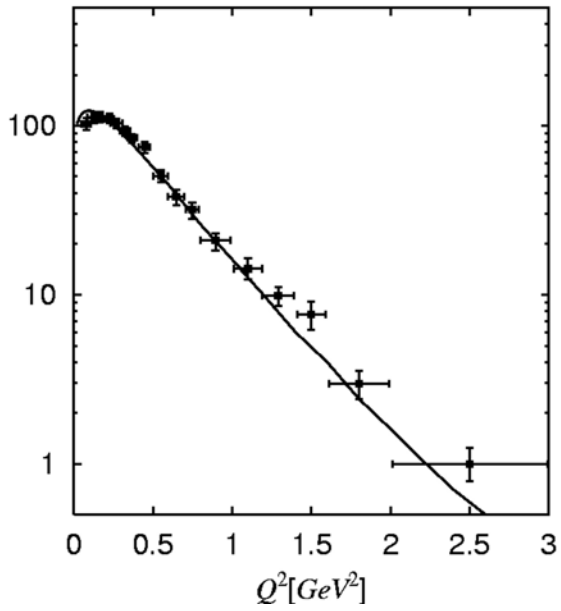

Fig. V-5b. The differential cross sections $d\sigma/dQ^2$ of $p(\nu,\mu^-\pi^+)$ reaction.

form factor contains large dynamical pion cloud effects, and these renormalization effects are crucial in getting agreement with the data. We conclude that the N-Δ transitions predicted by the constituent quark model are consistent with the existing neutrino-induced pion production data in the Δ region, contrary to previous observations. This is consistent with our previous findings in the study of pion electroproduction reactions. However, more extensive and precise data of neutrino-induced pion production reactions are needed to further test our model and to pin down the Q^2-dependence of the axial vector N-Δ transition form factor.

*Osaka University, Japan.

[1]Toru Sato and T-S. H. Lee, Phys. Rev. C **63**, 055201 (2001).

a.18. One-loop Corrections to Vector Meson Photoproduction Near Threshold

(T.-S. H. Lee and Y. Oh*)

One-loop corrections to ω photoproduction near threshold were investigated by using the approximation that all relevant transition amplitudes are calculated from the tree diagrams of effective Lagrangians. With the parameters constrained by the data of $\gamma N \to \pi N$, $\gamma N \to \rho N$, and $\pi N \to \omega N$ reactions, it is found that one-loop effects due to the intermediate πN and ρN states can significantly change the differential cross sections and spin observables. This is illustrated in Fig. V-6. The results from this investigation suggest strongly that the coupled-channel effects should be taken into account in extracting reliable resonance parameters from vector meson photoproduction data in the resonance region. A paper describing our results was published.[1] We have extended our approach to also investigate ρ and φ photoproduction reactions and found that the one-loop 2-π exchange mechanisms can replace the conventional, phenomenological σ-exchange in explaining existing data.

*Yonsi University, Seoul, Korea.

[1]Yongseok Oh and T.-S. H. Lee, Phys. Rev. C **66**, 045201 (2002).

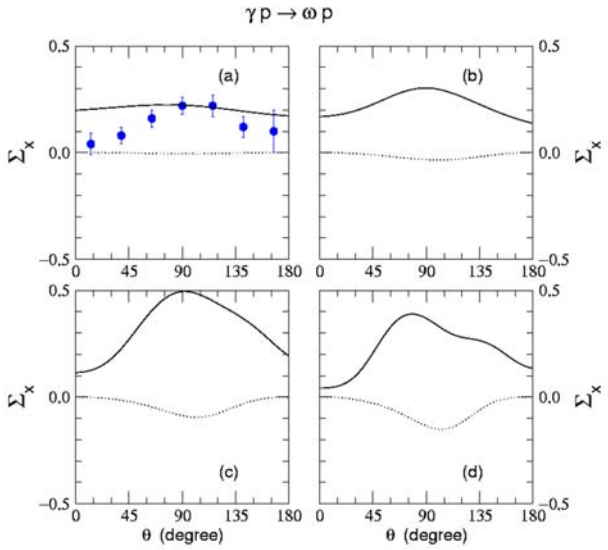

Fig. V-6. Single photon asymmetry Σ_x for $\gamma p \to \omega p$ at E_γ = 1.125 GeV (a), 1.23 GeV (b), 1.45 GeV (c), and 1.68 GeV (d). The dotted curves are from neglecting one-loop corrections.

a.19. Effective Lagrangian Approach to ω Photoproduction Near Threshold

(T.-S. H. Lee and Alexander I. Titov*)

We apply the effective Lagrangian approach to investigate the role of nucleon resonances in ω-meson photoproduction at energies near threshold. The nonresonant amplitudes are taken from previous investigations at higher energies and consist of the pseudoscalar meson exchange and nucleon Born terms. The resonant amplitudes are calculated from effective Lagrangians with the $N^* \to \gamma N$ and $N^* \to \omega N$ coupling constants fixed by empirical helicity amplitudes and the vector meson dominance model. The contributions from nucleon resonances are found to be significant in changing the differential cross sections in a wide interval of *t* and various spin observables. In particular, we suggest that a crucial test of our predictions can be made by measuring single- and double-spin asymmetries. A paper describing our results was published.[1]

*JAERI, Tokai, Japan.

[1]Alexander I. Titov and T.-S. H. Lee, Phys. Rev. C **66**, 015204 (2002).

a.20 Coherent ϕ and ω Meson Photoproduction from Deuterium and Nondiffractive Channels (T.-S. H. Lee, A. I. Titov,* and M. Fujiwara†)

For coherent photoproduction of ϕ and ω mesons from deuterium at forward angles, the isovector π-exchange amplitude is strongly suppressed. We show a possibility to study the nondiffractive channels associated with unnatural parity exchange in ϕ photoproduction and with baryon resonance excitations in ω photoproduction by measuring the spin observables. A paper describing our result was published.[1]

*JINR, Dubna, Russia, †Osaka University, Japan.
[1]A. I. Titov, M. Fujiwara, and T.-S. H. Lee, Phys. Rev. C **66**, 022202(R) (2002).

a.21. η Meson Production in NN Collisions (T.-S. H. Lee, K. Nakayama,* and J. Speth†)

η meson production in both proton-proton and proton-neutron collisions is investigated within a relativistic meson exchange model of hadronic interactions. It is found that the available cross section data can be described equally well by either the vector or pseudoscalar meson exchange mechanism for exciting the $S_{11}(1535)$ resonance. It is shown that the analyzing power data can potentially be very useful in distinguishing these two scenarios for the excitation of the $S_{11}(1535)$ resonance. A paper describing our results was published.[1]

*University of Georgia, †Forschungszentrum-Jülich, Germany.
[1]T.-S. H. Lee, K. Nakayama, and J. Speth, Phys. Rev. C **65**, 045210 (2002).

a.22. Study of Nucleon Resonances with Double Polarization Observables in Pion Photoproduction (T.-S. H. Lee, D. Dutta,* and H. Gao*)

Motivated by new experimental opportunities at Jefferson Lab, the role of nucleon resonances in the double polarization observables of pion photoproduction is investigated. As an example, we show that the not-well-determined two-star resonance $N^{-}_{3/2}(1960)$ can be examined by performing experiments on beam-recoil polarization at large angles. A paper describing our results was published.[1]

*Massachusetts Institute of Technology.
[1]T.-S. H. Lee, D. Dutta, and H. Gao, Phys. Rev. C **65**, 044619 (2002).

a.23 Spin Effects and Baryon Resonance Dynamics in ϕ-Meson Photoproduction at Few GeV (T.-S. H. Lee and A. I. Titov*)

The diffractive ϕ-meson photoproduction amplitude is dominated by Pomeron exchange but also contains terms that govern the spin-spin and spin-orbit interactions. We show that these terms are responsible for the spin-flip transitions at forward photoproduction angles and appear in the angular distributions of $\phi \to K^+K^-$ decay in reactions with unpolarized and polarized photon beams. At large momentum transfers, the main contribution to the ϕ-meson photoproduction is found to be due to the excitation of nucleon resonances. Combined analysis of ω and ϕ photoproduction indicates strong OZI-rule violation in ϕNN* couplings. We also show that the spin observables are sensitive to the dynamics of ϕ-meson photoproduction at large angles and could help distinguish different theoretical models of nucleon resonances. Predictions for spin effects in ϕ-meson photoproduction are presented for future experimental tests. A paper describing our results was submitted for publication.

*Japan Atomic Energy Research Institute, Tokai.

a.24. Unitary ππN Model for Investigating N* Resonances (T.-S. H. Lee, A. Matsuyama,* and T. Sato†)

In the second and third resonance regions, the πN and γN reactions involve three-body ππN channel in addition to various stable two-body channels such as ηN, ωN, and KΛ. To interpret the data in these energy regions correctly in terms of N* excitations predicted by various hadron models, it is essential to account for the ππN unitarity cut in any coupled-channel approach. We achieved this by developing a unitary coupled-channel ππN dynamical model with interactions derived by using the unitary transformation method. The numerical techniques needed for solving the resulting coupled integral equations were developed. In a model calculation including πN, πΔ, and ρN channels, we show that the ππN unitary condition has very large effects on πN reaction cross sections. We are now carrying out realistic calculations with N* in the S_{11} channel, aimed at exploring whether the empirical πN and γN amplitudes in this partial wave are consistent with the constituent quark model predictions.

*Shizuoka University, Japan, †Osaka University, Japan.

a.25. Quark-exchange Mechanism of γd → np Reaction at 2-6 GeV (T.-S. H. Lee and B. Julia-Diaz*)

Within the constituent quark model, we examine the extent to which deuteron photodisintegration at 2-6 GeV can be described by the quark-exchange mechanism. The main feature of our approach is an exact loop-integration over the exchanged quark propagator. With the parameters constrained by *np* scattering data up to 12 GeV, the calculated differential cross sections disagree with the data in both magnitude and energy-dependence. The results can be improved greatly if we use a smaller size parameter for quark wave functions. We find that the on-shell approximation used by others in previous investigations of the quark-exchange mechanism is not valid. This is illustrated in Fig. V-7. We also find that the predicted cross sections are sensitive to the mass parameters in the quark and gluon propagators. It is important to account for the momentum-dependence of these parameters in this energy region where the transition from the hadronic picture to the quark-gluon picture is taking place. A paper describing our results is being prepared for publication.

*University of Salamanca, Spain.

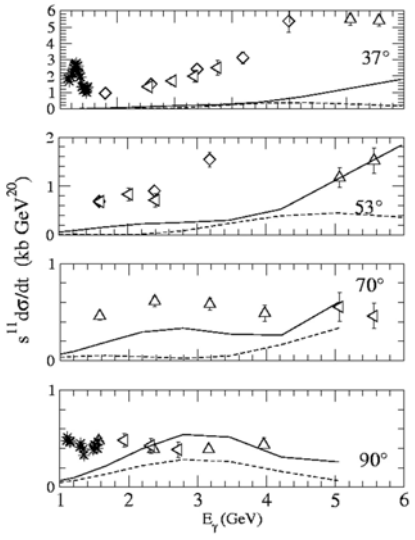

Fig. V-7. The γd → np differential cross sections. The solid curves are from exact loop integration, while the dashed curves are from taking the on-shell approximation used in previous investigations.

a.26. Locality in Relativistic Quantum Mechanics[1] (F. Coester)

The fundamental requirements of relativistic quantum theory are: 1) Implementation of relativistic space-time symmetry, realized by unitary representations of the Poincaré group, and 2) Einstein causality, which requires an appropriate definition of states localized in finite space-time regions. Implementation of the locality requirements is discussed extensively in the literature in the context of the algebraic formulation of quantum field theories. The basic ingredients are operator algebras, nets of localized sub-algebras with the covariance, union, intersection and inclusion properties of the associated space-time regions. "Essentially localized" state vectors are obtained by application of local operators to the vacuum state. Essential features of this framework are infinitely many degrees of freedom and inequivalent Hilbert-space representations of the states depending on the dynamics. Finite systems necessarily appear as subsystems of infinite systems.[1] In relativistic quantum mechanics the emphasis was on the implementation of the Poincaré symmetry by unitary representations of the Poincaré group on the Hilbert space of states, which is a finite tensor product of irreducible representations (single-particle states), or a finite direct sum of such spaces. The Poincaré generators can be expressed as functions of kinematic operators and the mass operator which specifies the dynamics. The choice of the kinematic operators determines the form of kinematics, that is a subset of generators which are independent of the mass operator. Einstein causality is realized asymptotically by the properties of cluster separability. Recent mathematical developments indicate how manifolds of localized states can be defined strictly within the framework of relativistic quantum mechanics without reference to infinite systems. This construction involves the domains of unbounded operators defined as functions of the Poincaré generators.

[1] F. Coester, Few Body Systems Suppl. **14** (2003).

a.27. Current Density Operators in Relativistic Quantum Mechanics[1] (F. Coester)

Relativistic quantum mechanics is a mathematically well-defined framework for the description of few nucleons, few hadrons and/or few constituent quarks for a limited range of the total mass spectrum. The Hilbert space of states consists of irreducible representation spaces of the Poincaré group (single-particle states), finite tensor products of single particle states, and finite direct sums of such tensor products, which is the same for interacting and noninteracting systems. The dynamics is specified by a unitary representation of the Poincaré group which may be identical to the representation of noninteracting constituents for a kinematic subgroup. The "form of kinematics" depends on the choice of that subgroup. Within this framework the dynamics generates fully covariant conserved currents from current density operators that are covariant under the kinematic subgroup. The choice of the form of kinematics implies important qualitative differences, which can be illustrated by simple toy models.

[1] F. Coester, Few-Body Systems Suppl., to be published.

B. NUCLEAR FORCES AND NUCLEAR SYSTEMS

The goal of this program is to achieve a description of nuclear systems ranging in size from the deuteron and triton to nuclear matter and neutron stars using a single parameterization of the nuclear forces. Aspects of our program include both the construction of two- and three-nucleon potentials and the development of many-body techniques for computing nuclear properties with these interactions. Detailed quantitative, computationally-intensive studies are essential parts of this program.

Quantum Monte Carlo (QMC) calculations of light ($A \leq 10$) nuclei with realistic interactions have been the main focus of our recent efforts. Our nonrelativistic Hamiltonian contains the accurate Argonne v_{18} two-nucleon (*NN*) potential, which includes charge-independence breaking terms, and either the venerable Urbana IX three-nucleon (*NNN*) potential, or one of several new Illinois *NNN* models. The QMC calculations include both variational (VMC) and Green's function (GFMC) methods. We begin with the construction of variational trial functions based on sums of single-particle determinants with the correct total quantum numbers, and then act on them with products of two- and three-body correlation operators. Energy expectation values are evaluated with Metropolis Monte Carlo integration and parameters in the trial functions are varied to minimize the energy. These optimized variational wave functions can then be used to study other nuclear properties. They also serve as a starting point for the GFMC calculations, which systematically remove higher excited-state components from the trial wave functions by propagation in imaginary time.

We are currently studying all $A \leq 10$ nuclei with experimentally known bound state or resonance energies, including ≈ 60 excited states. These are the first calculations treating $A \geq 6$ nuclei directly with realistic *NN* and *NNN* interactions. In GFMC calculations, with the new Illinois *NNN* models, we can reproduce most of the experimental ground- and excited-state energies within 0.7 MeV. In the last year we found that GFMC propagation started with orthogonalized VMC wave functions for several states of the same J^{π} preserves the orthogonality to a very good approximation. This enabled the calculation of many more states for $A \leq 10$, in previous years only some 30 states were done. We also made a study of the sensitivity of the binding energies to various features of the *NN* potential. We find that a complicated potential, including tensor and spin-orbit terms, is needed to reproduce such critical experimental features as the non-existence of bound 5- and 8-body nuclei. In another study we showed that modern nuclear Hamiltonians cannot produce a bound tetraneutron, despite a recent claimed experimental observation. Finally, we are also studying the properties of neutron drops with the goal of providing additional constraints for the construction of Skyrme interactions that are used in the modeling of neutron-rich nuclei in neutron star crusts.

Efforts using the coupled cluster [exp(S)] method also continued last year. The coupled cluster method is being used to study nuclei in the ^{12}C-^{16}O range, using the same realistic Hamiltonian as the quantum Monte Carlo calculations. Comparisons of GFMC and exp(S) results are being made for ^{4}He and neutron drops. We are also able to compare both methods with results of traditional shell model calculations. Lastly, studies of hypernuclei are also continuing, particularly the charge-symmetry-breaking of ΛN interactions.

b.1. Quantum Monte Carlo Calculations of Light p-shell Nuclei (S. C. Pieper, R. B. Wiringa, J. Carlson,* V. R. Pandharipande,† and K. Varga‡)

Since the early 1990s, we have been studying the ground and low-lying excited states of light p-shell nuclei as *A*-body problems with realistic nucleon-nucleon (*NN*) and three-nucleon (*NNN*) interactions using advanced quantum Monte Carlo (QMC) methods. Our preferred Hamiltonians contain the Argonne v_{18} *NN* potential (AV18), which gives an excellent fit to elastic *NN* scattering data and the deuteron energy and Illinois *NNN* potentials, which we have fit to binding energies of $A \le 8$ nuclei. The QMC methods include both variational Monte Carlo (VMC), which gives an initial approximate solution to the many-body Shrödinger equation, and the Green's function Monte Carlo (GFMC), which systematically improves on the VMC starting point and produces binding energies that are accurate to within 2%. In recent years we concentrated on $A = 9,10$ nuclei, and we are now making preliminary calculations of ^{12}C.

The VMC calculations begin with the construction of an antisymmetric Jastrow trial wave function that includes single-particle orbits coupled to the desired *JM* values of the state of interest as well as pair and triplet spatial correlations. It is then acted on by a symmetrized product of two-body spin, isospin, tensor, and spin-orbit correlation operators, induced by the *NN* potential, and three-body correlation operators for the *NNN* potential. The wave functions are diagonalized in the small basis of different Jastrow spatial symmetry components to project out higher excited states with the same quantum numbers.

In the GFMC calculations, we operate on a version of the VMC trial function with the imaginary time propagator, $\exp[-(H'-E_0)\tau]$, where H' is a simplified Hamiltonian, E_0 is an estimate of the eigenvalue, and τ is the imaginary time. The excited-state components of the trial function will then be damped out for large τ, leaving the exact lowest eigenfunction with the quantum numbers of the input variational wave function. The expectation value of *H* is computed for a sequence of increasing values of τ to determine the convergence. Our H' contains a simplified, reprojected eight-operator version of the *NN* potential, AV8′, and the full *NNN* potential. The small correction, $H-H'$, is computed perturbatively. The many-body propagator is written as a symmetrized product of exact two-body propagators, with the *NNN* potential treated in lowest order.

In previous years we made significant improvements in the GFMC algorithms, especially in solving the fermion sign problem for nuclear systems. The method and program now seems stable but with the availability of increased computer time we are making more extensive tests. The computer resources (both CPU time and memory) required for these calculations increase exponentially with the number of nucleons. Therefore, progress to bigger nuclei usually requires a new generation of computers.

Our recent QMC work is described in the following subsections.

---

*Los Alamos National Laboratory, †University of Illinois, Urbana, ‡Oak Ridge National Laboratory.

b.2. Recent Progress in Quantum Monte Carlo Calculations (S. C. Pieper, R. B. Wiringa, and J. Carlson*)

This year, we finished and published an extensive set of calculations of natural-parity states in $A = 9,10$ nuclei.[1] These calculations used essentially complete *p*-shell basis sets for the Jastrow wave functions; in several cases this lowered our earlier (unpublished) energies by 1-2 MeV. The present state of our calculations, including newer results discussed below, is shown in Fig. V-8. There is generally good agreement of the results using the Illinois-2 *NNN* potential and the importance of a *NNN* potential is clearly shown.

Since then we have made use of large blocks of early-user time on the second phase of the NERSC Seaborg and on Argonne's new Jazz computer to make extensive tests of the reliability of the GFMC for $A = 8$-10. Specifically, we studied our use of an approximate propagator for the three-body potential. This approximation was developed and reported a number of years ago for lighter nuclei with the Urbana-IX *NNN* potential; in those cases it gave better than 1% accuracy. It appears that in larger nuclei with the Illinois potentials it can be less accurate, with errors up to 2%. This is unfortunate, because the three-body

propagator uses an increasing fraction of the total computational time as A increases. The most accurate propagator that we have takes twice as long as the approximate one. We are continuing to study this and make other tests of the reliability of GFMC for A = 8-10.

GFMC starts with a trial wave function of certain quantum numbers and propagates to the lowest-energy state that is not orthogonal to the starting wave function. In the process of constructing the starting wave function (previous section), a small diagonalization produces several orthogonal wave functions with the same quantum numbers. We found that GFMC propagation seems to maintain this orthogonality; the propagation results in stable excited-state energies and the propagated wave functions remain almost orthogonal to the other starting wave functions (we cannot compute the overlap of two different GFMC propagations at present). Thus we can now compute many second and higher states of the same quantum numbers in a given nucleus; so far, as shown in Fig. V-8, we are obtaining mostly good agreement with known experimental energies for these states. This work is also continuing.

Finally, we made use of the new Jazz computer at Argonne to make our first, preliminary, calculations of ^{12}C. These were first made with just the AV8' and AV18 *NN* potentials and then one calculation (40,000 2.4GHz Pentium-4 processor hours) was made using AV18 plus the Illinois-2 *NNN* potential. The starting wave function had just the ^{1}S[444] symmetry and so is certainly inadequate. Since then we expanded the program to also include a $(p_{3/2})^8$ basis state; this lowers the starting energy by only 1.2 MeV, but we do not know what effect it will have on the GFMC propagation. These preliminary calculations are also using the approximate three-body propagator discussed above. Thus more extensive calculations (requiring much more computer time) will be needed before a definitive result can be obtained.

*Los Alamos National Laboratory.

[1]S. C. Pieper, K. Varga, and R. B. Wiringa, Phys. Rev. C **66**, 044310/1-14 (2002).

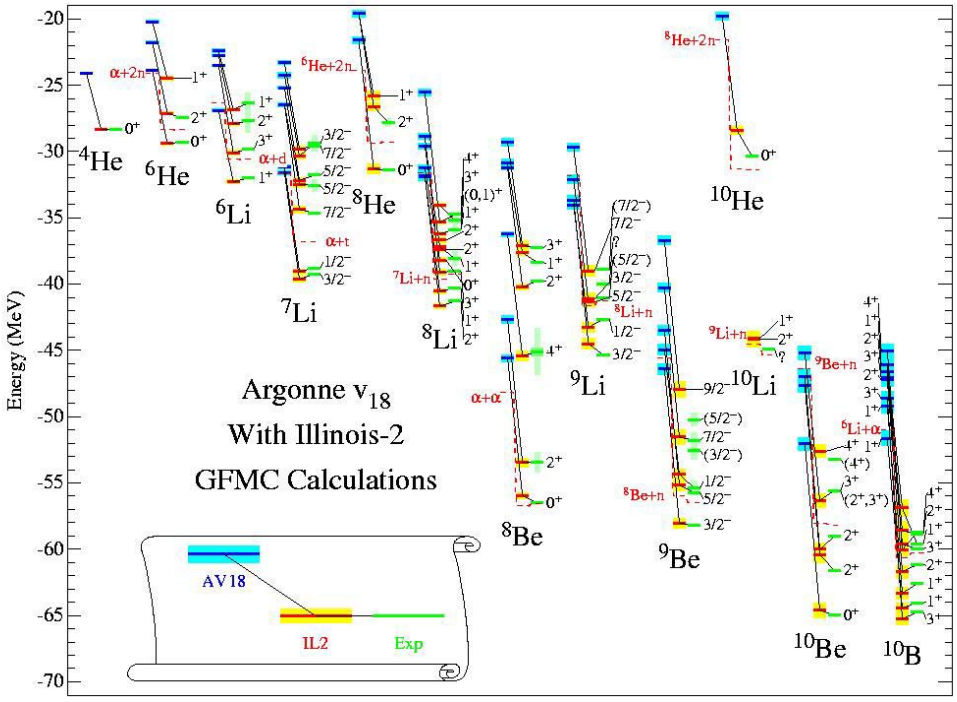

Fig.V-8. GFMC energies for A = 4-10 nuclei using the AV18 NN potential by itself and with the Illinois-2 NNN potential, compared to experiment.

b.3. Evolution of Nuclear Structure with Nuclear Forces (R. B. Wiringa and S. C. Pieper)

One of the most intriguing features of light nuclei is the absence of stable five- and eight-body systems. This fact is of enormous importance for the chemical evolution of the universe, limiting big bang nucleosynthesis to elements no heavier than lithium, while giving stars like our sun a long lifetime during which biological evolution can take place. In this work we studied what aspects of nuclear forces are necessary to obtain observed nuclear spectra, *i.e.*, the binding and relative stability of light nuclei, including the crucial mass gaps at A = 5 and 8.

We know from our quantum Monte Carlo (QMC) studies of light nuclei that a realistic two-nucleon potential, like Argonne v_{18} (AV18), that accurately reproduces NN scattering data, is unable to reproduce nuclear binding energies precisely without the addition of a fairly sophisticated three-nucleon force, such as one of the Illinois models. Nevertheless, AV18 by itself does produce reasonable nuclear spectra, with ^{5}He unstable against breakup into ^{4}He + n and ^{8}Be unstable against breakup into ^{4}He + ^{4}He. It also gives a fairly good ordering of low-lying excited states, although some weakly bound nuclei, like ^{6}He and ^{8}He are not predicted to be stable.

We constructed a series of progressively simpler two-nucleon potentials to see what aspects of the nuclear force are crucial to these stability issues. The first simplification is AV8', a reprojected version of AV18 retaining central, spin, isospin, tensor, and spin-orbit forces, but dropping quadratic momentum-dependent and charge-independence-breaking terms. AV8' reproduces the charge-independent average of *S*- and *P*-wave phase shifts and the deuteron properties of AV18 using eight operators instead of eighteen. QMC calculations of the light nuclei show that the spectra from AV8' are shifted to slightly greater binding than AV18, but overall are very similar.

We dropped the spin-orbit terms and readjusted the remaining six operators (to preserve the deuteron binding) to create an AV6' model. This model still fits *S*-wave phases well, but no longer reproduces $^3P_{0,1,2}$ partial waves. It does have mass gaps at A = 5 and 8, but the intervening ^{6,7}Li nuclei are not clearly stable. Eliminating tensor terms, and again adjusting the remaining four operators (to preserve deuteron binding), we produced an AV4' model. This force gives ^{8}Be more than twice as bound as ^{4}He, so the A = 8 mass gap has disappeared, although A = 5 nuclei are still unstable. Finally, we eliminate additional operators, producing AV2' and AV1' models, which retain the features of a repulsive core and intermediate-range attraction. However, these models provide no saturation in the light p-shell nuclei, predicting ever-increasing binding as nucleons are added. The purely central AV1' model would predict that the most stable nuclei up to A = 10 are the series of helium isotopes.

We conclude from this study that the A = 5 and 8 mass gaps require a combination of spin-isospin exchange forces and tensor forces, and that stability of the intervening A = 6,7 nuclei probably also requires spin-orbit forces. Thus the nature of the universe we live in is crucially dependent on the complicated nature of the *NN* interaction that we actually observe in the laboratory. This work was published as a Physical Review Letter[1] and featured online in Physical Review Focus.

[1] R. B. Wiringa and S. C. Pieper, Phys. Rev. Lett. **89**, 182501, 1-4 (2002).

b.4. Can Modern Nuclear Hamiltonians Tolerate a Bound Tetraneutron? (S. C. Pieper)

A recent experimental paper reported the apparent observation of bound tetraneutrons. This inspired a number of approximate calculations by several authors, using simplified forces, of the energy of ^{4}n; the conclusions were that ^{4}n is unbound. I have completed more reliable calculations, using GFMC with the AV18 + Illinois-2 Hamiltonian, of ^{4}n. These show that for such a realistic force ^{4}n is not bound, but might have a (probably very broad) resonance at +2 MeV. I also made calculations using some of the simplified models (Volkov potentials) that other authors had used approximately. My results are that the Volkov potentials (which are known to have a bound dineutron) result in ^{4}n with negative energies, although the ^{4}n energy is still above the energy for breakup into two dineutrons; the previous results had not indicated the possibility of such a low energy.

A number of modifications of the AV18 + Illinois-2 Hamiltonian were made to force ^{4}n to have a energy of about -0.5 MeV. The resulting Hamiltonians were then used to compute the energies of other light nuclei. Some of the results are shown in Fig. V-9. In all cases the modifications result in dramatic disagreements with other experimental energies. For example, if the binding of the ^{4}n is achieved by modifying the $^1S_0$ part of AV18 (the only channel that will achieve such binding), then the dineutron becomes bound by about the same amount so that, in fact, the ^{4}n can still break into two dineutrons. This results in a large change in the experimentally well determined $^1S_0$ phase shifts. Furthermore, ^{3}H becomes overbound by 50% and other light nuclei also become very overbound.

It was suggested that three- or four-neutron potentials could bind ^{4}n; such potentials would not affect any two-nucleon properties. By making the potentials act only in isospin 3/2 or 2 channels, effects on some nuclei (like ^{3}H or ^{4}He) can also be avoided. However, it turns out that the potentials must be made quite strong to produce a minimally bound ^{4}n. As is shown in Fig.V-9, this results in large changes to the binding energies of any nucleus in which the potential can have non-zero expectation value; in particular the most bound A = 6, 8 systems are pure neutron systems! Thus it appears that should the experimental claim of a bound ^{4}n be confirmed, our current very successful understanding of nuclear forces would have to be severely modified. This work was submitted for publication.

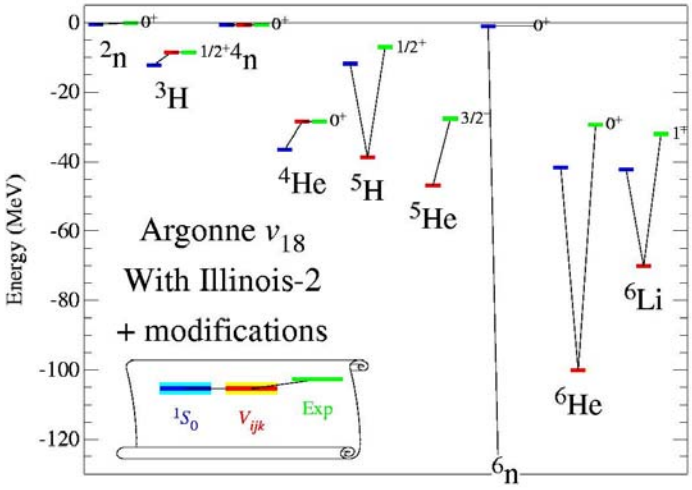

Fig. V-9. Comparison with experiment of energies of light nuclei using modified Hamiltonians. Left (blue) bars obtained by modifying the $^1S_0$ part of AV18, middle (red) bars obtained with an additional T = 3/2 NNN potential; both changes were chosen to give a ^{4}n with about -0.5 MeV energy.

b.5. Pairing and Spin-orbit Splitting in Neutron Drops (S. C. Pieper and V. R. Pandharipande*)

Systems of neutrons interacting with realistic forces are unbound. However, bound systems may be made by adding an artificial external well to the Hamiltonian. These may then be used to study spin-orbit splitting and pairing energies in neutron-rich systems and to possibly provide "experimental" energies to help constrain Skyrme models for large neutron-rich nuclei. A number of years ago we published results for 7 and 8 neutrons interacting via AV18 + Urbana IX in an external well and the corresponding 6-neutron system was also published.

We are now studying from 1 to 10 neutrons, all in the same well, interacting with several Hamiltonians. Some preliminary results are shown in Fig. V-10. The well is the same one that was used before and is strong enough to bind one or two neutrons (*s*-shell) but not to bind a *p*-wave neutron. Thus the binding of 3-8 neutrons arises only from the combined effects of the nuclear Hamiltonian and the external well. The 9-neutron system is not bound (the ^{9}n($\frac{1}{2}^+$) energy is slightly above the ^{8}n energy); calculations have not yet

been made for ^{10}n. One can see that the spin-orbit splitting gradually increases as the *p*-shell is filled (from 3 to 7 neutrons) and then becomes dramatically smaller for the *d*-shell in 9 neutrons. The staggering of the ^{2,3,4}n, ^{4,5,6}n, and ^{6,7,8}n energies shows the pairing energies. This work is continuing.

*University of Illinois, Urbana-Champaign.

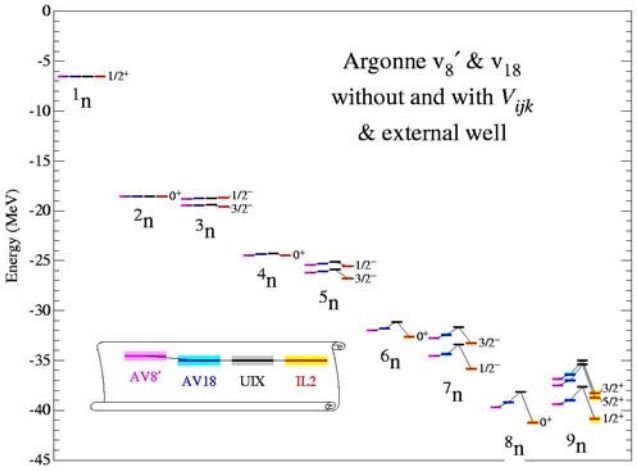

Fig. V-10. Energies of neutron systems interacting with the indicated Hamiltonians and an artificial external Woods Saxon well (V=20 MeV, R=3.0 fm, a=0.65 fm).

b.6. Quadratic Momentum Dependence in the Nucleon-Nucleon Interaction

(R. B. Wiringa, A. Arriaga,* and V. R. Pandharipande†)

Modern nucleon-nucleon (NN) interactions all start with eight basic operators, including central, spin-spin, tensor, and spin-orbit terms, and each of these times isospin-isospin. With these operators it is possible to fit S- and P-wave phase shift data and deuteron properties reasonably well, as evidenced by the AV8' potential model. However, to fit higher partial waves, *e.g.*, the difference between $^1S_0$ and $^1D_2$ partial waves, it is necessary to add operators with a quadratic momentum dependence (QMD). An example is the use of four L^2 and two $(L\cdot S)^2$ operators in the AV18 potential.

There are other possible choices for the QMD terms, *e.g.*, p^2 instead of L^2 operators, and different kinds of quadratic spin-orbit terms. One advantage of the AV18 operators is that the potential is local, since L^2 commutes with functions of radial coordinates. However, potentials based on field-theoretic models of meson-exchange are more likely to have p^2 terms, as in the Bonn, Nijmegen, and Paris potentials. The p^2 operator does not commute with functions of r and consequently such models are nonlocal, and somewhat harder to evaluate in our quantum Monte Carlo many-body calculations. Nevertheless, there is evidence that such nonlocal potentials can provide somewhat more attraction in light nuclei, such as ^{3}H and ^{4}He.

We are studying the effect of such nonlocality in the NN potential model by making a phase-equivalent variant of AV18 where L^2 operators were converted to p^2 operators. The magnitude of these terms is constrained by the need to fit higher partial waves. Initial VMC results suggest that the nonlocal variant, which we call AV18pq, is indeed slightly more attractive in the light nuclei: 140 keV in ^{3}H and 420 keV in ^{4}He. However, these nuclei are still underbound compared to experiment, calling for the addition of a three-nucleon (*NNN*) potential. When the Urbana IX (UIX) *NNN* potential is added, the extra attraction of the nonlocal potential is greatly reduced; in fact the AV18/UIX and AV18pq/UIX Hamiltonians give identical binding energies for ^{4}He. Thus it appears that this kind of nonlocality has little practical effect on ground state energies.

*University of Lisbon, Portugal, †University of Illinois at Urbana-Champaign.

b.7. The Three-Body Interaction in Mean-Field Calculations (T. Duguet, R. B. Wiringa, and S. C. Pieper)

Three-body forces were proven crucial to obtain good saturation properties in nuclear matter, to describe spectroscopic properties of light nuclei in *ab-initio* calculations, and to the treatment of nucleon-induced deuteron break-up or nucleon-deuteron elastic scattering. However, self-consistent mean-field calculations of (heavier) finite nuclei include the effect of three-body forces only in a very schematic way. As a result, we would like to propose a three-body interaction based on realistic three-body forces derived from meson-exchange field theory to be used in self-consistent mean-field methods. The challenge is to obtain a form which is simple enough to be tractable but which does not give up the essential physics contained in each channel of the interaction. For instance, one has to reconcile the crucial binding effect of the three-body force in light nuclei with its saturation character at the normal density of nuclear matter. Our experience from the calculations of light nuclei with realistic forces will be of great help for this purpose.

b.8. Coupled-Cluster Expansion Approach to Nuclear Structure (B. Mihaila and J. Heisenberg*)

We continued our project on developing a realistic description of the ground-state of closed-shell nuclei in the p-shell (^{12}C and ^{16}O). These calculations use the coupled-cluster expansion (CCE), together with a realistic nuclear interaction and currents. Just as the GFMC method, the CCE approach is an exact approach to solving the nuclear many-body problem. The present calculations are done in configuration space, and suffer from limitations due to the intrinsic cutoffs one has to impose when defining the model space. The single-particle states are expanded out in an harmonic oscillator basis, and satisfy the same type of boundary conditions for both the hole and particle states. In effect we discretize the continuum part of the one-body mean-field Hamiltonian used to define the single-particle spectrum. This results in the necessity of a large configuration space and subsequent significant storage problems and lengthy execution time.

A new approach to solving the CCE equations is underway with a study of the nuclear matter problem. In the nuclear matter case we are dealing with the diametrically opposite case of a purely continuum system. In this work we are also pursuing a different approach to solving the CCE equations, in which one avoids the direct calculation of the two-, three- (*etc*.) particle-hole excitations altogether, and rather concentrates on calculating expectation values in a formalism reminiscent of GFMC for finite nuclei. The new approach is well-suited for implementation on massively parallel multiprocessor machines. We believe that the experience acquired in this process will provide significant insight into new ways of approaching the CCE equations for finite systems.

*University of New Hampshire.

C. NUCLEAR STRUCTURE AND HEAVY-ION REACTIONS

This research focuses on nuclear structure in unusual regimes: nuclei far from stability, and superdeformed nuclei at high spin. We also study heavy-ion reactions near the Coulomb barrier. Much of this work is closely tied to experiments performed at ATLAS and at radioactive beam facilities.

Our studies of drip-line nuclei focus on breakup reactions, induced by the Coulomb and nuclear fields from a target nucleus. A critical issue is to develop a realistic description of the breakup mechanisms as a necessary tool for extracting nuclear structure properties of drip-line nuclei. We applied our numerical technique of calculating the time-evolution of the two-body wave function for the relative motion of a halo nucleon and a core nucleus, in the time-dependent fields from a target nucleus. Our results are used to test the validity of simpler reaction models and to analyze related experiments.

Our numerical studies of the Coulomb dissociation of proton halo nuclei on high-Z targets show that the conventional first-order perturbation theory for distant collisions is a poor approximation at low energy. The leading order correction is a dynamic polarization effect, which reduces the dissociation probability. A further complication for loosely bound nuclei such as ^{8}B is the influence of close collisions, where projectile and target have a non-zero overlap during the collision. Our calculations are consistent with low energy measurements of the one-proton removal from ^{8}B and ^{17}F.

We applied our coupled-channels technique to study heavy-ion fusion reactions. The primary goal is to develop a good understanding of the energy dependence of the fusion cross section, in particular at extreme sub-barrier energies, where measurements are difficult so one has to rely on extrapolations.

Some nuclear structure problems, with which we are involved, are superdeformation, heavy and superheavy elements, proton radioactivity, the neutron deficient Pb region and neutron-proton pairing near the N = Z line. To study these problems we make use of (1) the Strutinsky method as well as (2) self-consistent mean field (SCMF) calculations using the Gogny interaction, and (3) many-body (MB) wave functions.

In nuclides with roughly equal number of protons and neutrons, T = 1 and T = 0 n-p pairing will play an important role, in addition to the usual like-nucleon T=1 pairing. To adequately treat and understand these effects, it is necessary to go beyond the quasiparticle approximation and to study not only those nuclei that are exactly on the N = Z line. The rare isotope accelerator (RIA) will provide considerable spectroscopic information on nuclides near the N = Z line. We extended our many-body code to include neutron-proton pairing interactions. We found that there is a new quantum number for characterizing collective states; *i.e.*, the number parity of the T = 0 and T = 1 n-p pairs. In addition to the collective states, there are states in which some levels are 'blocked', *i.e.* have an odd number of nucleons in the level. All states in odd mass nuclei fall into this category. Also, the ground states of odd-odd nuclei are more likely to be of this type as the neutron excess increases. We extended our method to include states of this type and studied the structure of low-lying states in odd-odd nuclei. Our studies of superdeformation

at both low and high spins address the issue of possible new regions of superdeformation and hyperdeformation. Special emphasis is placed on the study of fission barriers at high spin as this is crucial for the possible production of very extended nuclei.

c.1. Dynamic Polarization in the Coulomb Dissociation of ^{8}B (H. Esbensen and G. F. Bertsch*)

We calculated the dissociation of ^{8}B to all orders in the Coulomb field from high-Z targets.[1] The motivation is to test the validity of first-order perturbation theory, and to determine the magnitude of the dynamic polarization effect, which we observed in previous calculations of the Coulomb dissociation of ^{17}F at low beam energies.[2] The ground state of ^{8}B is modeled as a two-body system, consisting of a proton and a ^{7}Be core and bound as a p-wave in a Wood-Saxon well. The relative motion of projectile and target is described by a classical Coulomb trajectory. The time evolution of the ^{8}B two-body system in the Coulomb field from a target nucleus is obtained by solving the time-dependent Schrödinger equation numerically.

The leading order correction to first-order perturbation theory is of order Z^3 in the target charge Z. It is caused by a dynamic polarization where the wave function of the proton-core system has time to adjust itself during the collision with the target. Corrections that are odd in Z can be isolated from the numerical calculations simply by repeating them with a negative target charge. Denoting the two Coulomb dissociation probabilities by $P^{(+)}$ and $P^{(-)}$, for a positive and negative target charge, respectively, one can then define the charge asymmetry ratio

$$B = \left[p^{(+)} - p^{(-)} \right] / \left[p^{(+)} + p^{(-)} \right].$$

One can parameterize the charge asymmetry ratio to leading order in Z as

$$B = \frac{CZe^2}{E_{beam}\sqrt{b^2 + a^2}} \left(\frac{40}{E_{beam}} \right)^{\nu},$$

as function of beam energy (per nucleon) and impact barameter b. The coefficients we obtain for ^{8}B are C = -1.25, a = 37 fm, and v = 0.07. The dynamic polarization can cause a substantial reduction in the dissociation probability. The reduction is up to 30% in the example illustrated below.

The conventional first-order Coulomb dissociation is based on Coulomb form factors that are strictly correct only for distant collisions, i.e., when projectile and target do not overlap during the collision. This is a very good approximation for stable nuclei but it becomes questionable for weakly bound halo states that have a large spatial extent. We find that the reduction due to close collisions sets in at impact parameters less than 25 fm in the case of ^{8}B on a nickel target. Moreover, this reduction is weakly-dependent of beam energy.

The combined effect of close collisions and dynamic polarization explains quite well lthe (^{8}B, ^{7}Be) breakup cross section that was measured at 3.2 MeV/u on a nickel target. The comparison with the data is shown in Fig. V-11. The top curve (a) is the result of the conventional first-order Coulomb dissociation for distant collisions. The dashed curve (b) is the first-order result one obtains by treating close collisions correctly. The dotted curve (c) is the full dynamical calculation of the Coulomb dissociation. The reduction of this curve compared to curve (b) is mainly due to the dynamic polarization. Finally, curve (d) is the total (^{8}B, ^{7}Be) cross section, obtained by also including the nuclear proton-target interaction in the calculation. The effect of a Coulomb-nuclear interference in the diffraction dissociation is surprisingly weak. The main reason that curve (d) is above curve (c) at large angles is the contribution from stripping. This work was published.[1]

*Institute for Nuclear Theory, University of Washington.

[1]H. Esbensen and G. F. Bertsch, Phys. Rev. C **66**, 044609 (2002).
[2]H. Esbensen and G. F. Bertsch, Nucl. Phys. **A706**, 383 (2002).

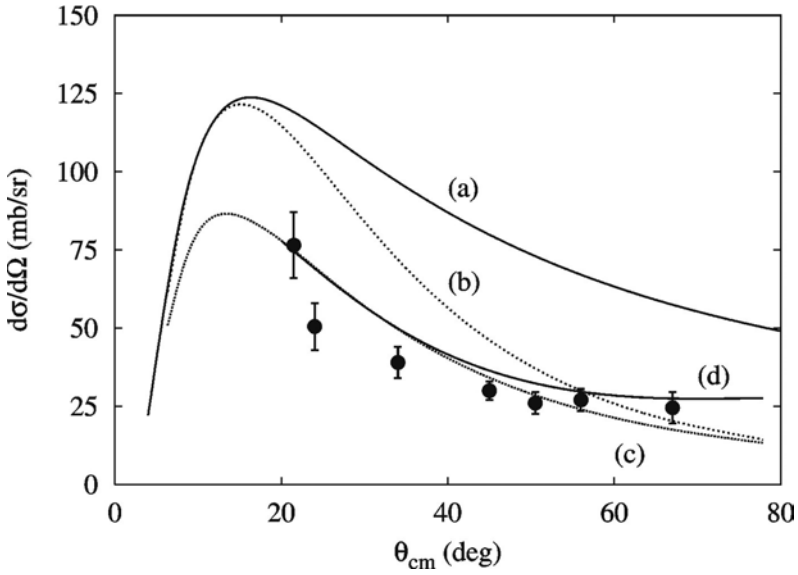

Fig. V-11. (^{8}B,^{7}Be) breakup at 26 MeV on a Ni target. The data are from V. Guimaraes et al., Phys. Rev. Lett. ***84****, 1862 (2000).*

c.2. Interplay of E1 and E2 Transitions in Multi-phonon Coulomb Excitation

(H. Esbensen and A. Volya)

The dynamic polarization effect, which we observed in numerical studies of the Coulomb dissociation of ^{17}F and ^{8}B, is of general interest because it occurs in other fields of physics. In atomic physics, for example, it leads to a difference in the stopping powers of protons and anti-protons. It is caused by the interplay of dipole (E1) and quadrupole (E2) transitions in higher-order processes.

The simplest system that can be used to illustrate the dynamic polarization is a three-dimensional harmonic oscillator that is perturbed by a time-dependent dipole and quadrupole Coulomb field from a heavy ion. In an effort to get more insight, we decided to study this system in more detail.[2] The excitation of harmonic oscillators by external, time-dependent fields that are linear and quadratic in the oscillator coordinates (or momenta) represents the most general quantum mechanical problem for which the dynamics is completely classical. In fact, by employing classical dynamics and Wigner transformations, which relate the classical phase space distribution and the quantum mechanical density matrix, it is possible to generate the excitation probabilities of interest, as discussed in Ref. 3.

We adopted a different approach in, Ref. 2, namely, to calculate the time evolution of the creation and annihilation operators in the Heisenberg representation. The transformation that relates these operators before and after the interaction is an example of a generalized Bogoliubov transformation. Thus we obtained an exact analytic expression for the total excitation probability in terms of a complex three-dimensional vector and a symmetric three-by-three matrix. These 9 complex amplitudes are determined by classical equations of motion. The vector is related to a displacement in the classical phase space; it is mainly generated by the E1 field but it also has contributions from the E2 field. In fact, it is the interplay between these two fields in the displacement vector that is responsible for the dynamical polarization. The three-by-three matrix, on the other hand, is generated entirely by the E2 field. In quantum optics, it is referred to as squeezing.[3]

The total excitation probability of an oscillator, perturbed by the Coulomb dipole and quadrupole fields from a heavy nucleus at a fixed impact parameter $b = 4$, is illustrated in Fig. V-12, as a function of velocity (in oscillator units). The parameters were chosen to simulate the excitation of ^{17}F on a nickel target. The solid curve in the middle is the result in first-order perturbation theory. The top and bottom curves are the exact results to all orders in the dipole and quadrupole fields, for an attractive and a repulsive interaction, respectively. The reduction/enhancement of the

probability for repulsive/attractive interactions compared to the first-order result is consistent with the findings for the Coulomb dissociation of ^{17}F in Ref. 1.

The simplicity of the analytic expression we have obtained for the total excitation probability allows us to discuss a quantum perturbation expansion in terms of iterative solutions for the 9 classical, complex amplitudes mentioned above. Thus we could easily extract the dynamic polarization effect as an interference between the dominant first-order dipole and a second order dipole-quadrupole amplitude. We have also discussed the influence of quadrupole transitions on the two-phonon dipole excitation. Most importantly, and in contrast to previous discussions of the dynamic polarization effect, our formulation provides the exact answer to all orders in the dipole and quadrupole fields. This work was published.[2] A further discussion of related phenomena in other branches of physics was accepted for publication.[3]

[1]H. Esbensen and G. F. Bertsch, Nucl. Phys. **A706**, 383 (2002).
[2]Alexander Volya and H. Esbensen, Phys. Rev. C **66**, 044604 (2002).
[3]Alexander Volya and H. Esbensen, J. Opt. B (in press 2003).

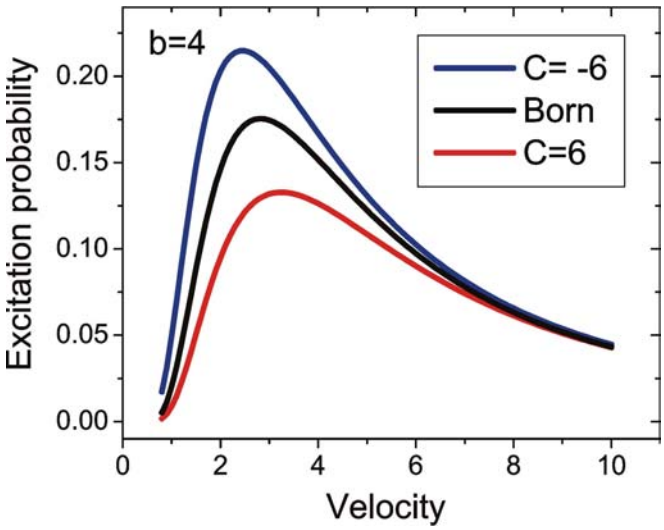

Fig. V-12. Total Coulomb excitation probability for repulsive (lowest curve) and attractive (highest curve) Coulomb interaction with a Ni target. The middle curve is the first-order result.

c.3. ^{17}F Breakup Reactions on Pb near the Coulomb Barrier (H. Esbensen, F. Liang,* and others*)

We applied our numerical methods[1] to calculating ^{17}F $\rightarrow$ ^{16}O + proton two-body breakup on a Pb target at low energies. This is done by solving the time-dependent Schrödinger equation for the ^{16}O+p two-body system in the Coulomb and nuclear fields from the target nucleus. The time-dependence of the fields is generated by assuming that the relative motion of projectile and target follows a classical Coulomb trajectory. The two-body Hamiltonian, which is based on a simple Woods-Saxon well, was adjusted to give the correct separation energy of ^{17}F and also a reasonable value of the S-factor for radiative proton capture on ^{16}O.

The results were compared to measurements at low energy on a Pb target. The first set of measurements was performed at 170 MeV and included singles events of oxygen fragments, and also events of oxygen fragments in coincidence with a proton.[2] The coincidence yield was surprisingly small in comparison to Coulomb dissociation. However, the measurement was performed at a large scattering angle, where nuclear interactions and a strong absorption set in. Including the proton-target nuclear interaction and also the effect of absorption of the ^{16}O fragment on the target, we obtained reasonable agreement with the measured proton-oxygen coincidences.

The angular distribution of oxygen fragments has a strong peak at grazing angles. The yield is much higher than the calculated cross section for proton transfer to

bound states in Bi. The total breakup cross section that we obtain in our two-body model of ^{17}F is in much better agreement with the data. It is dominated by proton stripping, which in the calculation is generated as an absorption by the imaginary proton-target interaction. The diffraction dissociation, where both the proton and the ^{16}O core fragment appear in the continuum after the collision, is a much smaller component at grazing angles, but it becomes the dominant component at forward angles. This work was published. [3]

The measurement of the angular distribution of oxygen fragments was repeated at 98 and 120 MeV.[3] One motivation for performing such measurements is to get data that can put constraints on speculations about the influence of breakup reactions on the yield of fusion. Unfortunately, our two-body model cannot predict the fusion because the relative motion of projectile and target is treated classically, and it is an input to the calculation. The model can only predict the breakup yield. An example at 120 MeV is shown in Fig. V-13. The measured elastic scattering (top part) is used to calibrate the absorption of the oxygen fragment; this absorption determines the falloff at large angles. The observed peak of oxygen fragments (bottom part) is reproduced quite well by the calculation (the solid curve), which again is dominated by stripping (the dotted curve). This work was accepted for publication.[3]

*Oak Ridge National Laboratory.

[1]H. Esbensen and G. F. Bertsch, Nucl. Phys. **A706**, 383 (2002).
[2]J. F. Liang *et al*., Phys. Rev. C **65**, 051603 (2002).
[3]J. F. Liang *et al*., Phys. Rev. C (in press 2003).

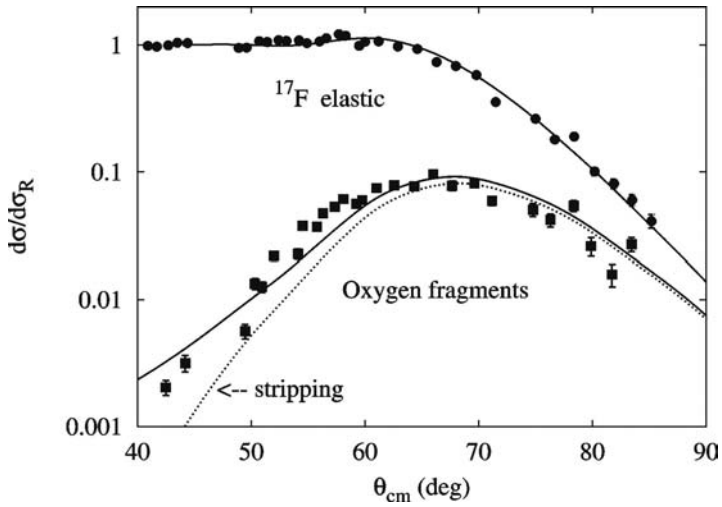

Fig. V-13. Elastic scattering and breakup of ^{17}F on a Pb target at 120 MeV.

c.4. Energy Dependence of ^{27}Al + ^{A}Ge Fusion at Sub-barrier Energies

(H. Esbensen and C. L. Jiang)

Theoretical and experimental studies of heavy-ion fusion have, in the past, focused on the energy dependence of cross sections near and slightly below the Coulomb barrier. One way to amplify certain features of the data is to extract the so-called barrier distribution, which is defined as the second derivative of cross section times energy, $B = d^2/dE^2(E\sigma_f)$. The goal has been to explain this distribution in terms of the structure of the reacting nuclei.

Not much attention was devoted to the energy dependence of cross sections far below the Coulomb barrier. In fact, many models assume that $E\sigma_f$ has a simple exponential dependence, as given by the Hill-Wheeler formula. Recently we pointed out[1] that the fusion cross sections for several systems exhibit a much steeper falloff at energies far below the Coulomb barrier. This feature is emphasized in the so-called logarithmic slope, $L(E) = d/dE[\log(E\sigma_f)]$. For several heavy-ion systems it appears that the value of $L(E)$

continues to grow steeply with decreasing energy, even far below the Coulomb barrier. Coupled-channels calculations, on the other hand, do not reproduce this behavior.

Here we chose to illustrate the low-energy behavior of *L(E)* by analyzing the rather accurate fusion data for ^{27}Al + ^{76}Ge that were reported in Ref. 2. Values of *L(E)* extracted from the measurement are shown in the Fig. V-14. The solid curve is the result of coupled-channels calculations that fit the measured fusion cross section quite accurately (with a $\chi^2 = 1.8$). The dotted curve in the middle shows the result of the one-dimensional barrier penetration, with a Coulomb barrier of 53.3 MeV. It increases steeply with decreasing energy in the vicinity of the Coulomb barrier but the rise levels off far below the barrier. The coupled-channels calculation has a similar behavior but is shifted a few MeV toward lower energies. In fact, the transition from the steep to the slower rise occurs at an energy where the barrier distribution *B(E)* goes to zero.

The modest rise in the calculated values of *L(E)* far below the lowest barrier is similar to what one obtains by assuming a constant S-factor. Thus with $E\sigma_f = S\exp(-2\pi\eta)$, where S is a constant S-factor and $\eta = Z_1Z_2e^2/(\hbar v)$ is the Sommerfeld parameter, one obtains $L(E) = \pi\eta/E$. This quantity is shown by the top dotted curve in Fig. V-14. It represents, in some sense, an extreme value of *L(E)* because a constant S-factor implies an s-wave penetration of the Coulomb potential all the way to $r = 0$. It is therefore surprising that values of *L(E)* extracted from some measurements can exceed the curve for constant S-factor.

The agreement between the coupled-channels calculation and measurements is very good in the case considered here. However, one cannot exclude the possibility that *L(E)* would steadily increase if measurements were performed at even lower energies, just as has been observed for other systems.[1] The general trend of the coupled channels calculations we have performed, on the other hand, is similar to that shown in the figure, namely, that the steepness of *L(E)* levels off below the lowest barrier. The analysis of fusion for other ^{27}Al + ^{A}Ge systems is in progress.

[1] C. L. Jiang *et al*., Phys. Rev. Lett. **89**, 052701 (2002).
[2] E. F. Aguilera *et al*., Phys. Rev. C **41**, 910 (1990).

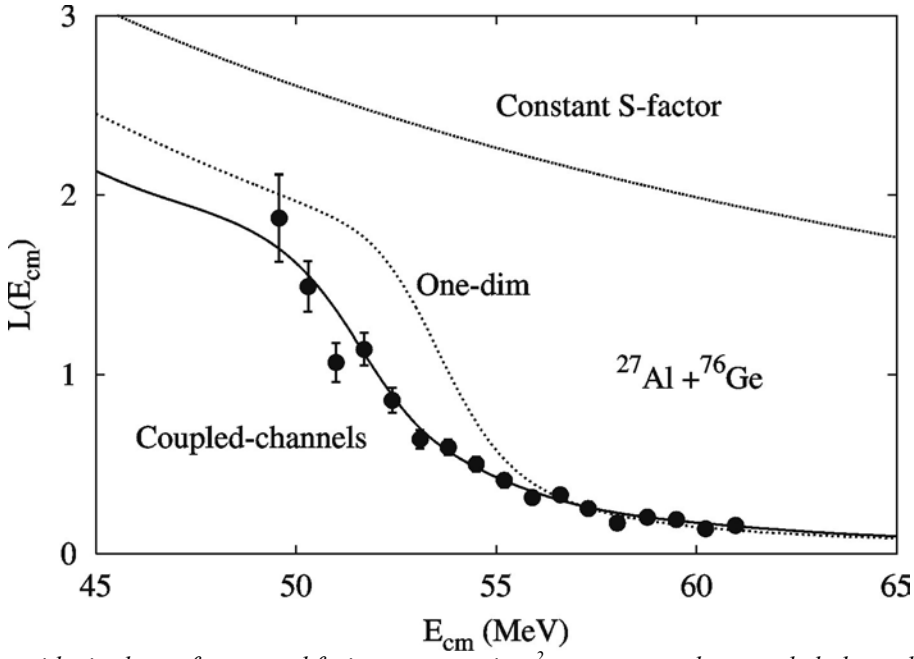

Fig. V-14. Logarithmic slope of measured fusion cross sections[2] are compared to coupled-channels calculations, one-dimensional barrier penetration, and to values for a constant S-factor.

c.5. Mean Field and Many Body Wave Functions (R. R. Chasman)

We are continuing the development of a program for calculating many-body variational wave functions that puts pairing and particle-hole two-body interactions on an equal footing. The complexity of the wave functions depends only on the number of levels included in the valence space. In these wave functions, we conserve particle number and parity strictly; projecting states of good particle number and parity before carrying out the variational calculations. We also extended the program to calculate the spectroscopic factors involved in proton decay. This is useful for studies of nuclides near the proton drip line.

By using residual interaction strengths (*e.g.*, the quadrupole interaction strength or pairing interaction strength) as generator coordinates, one gets many different wave functions; each having a different expectation value for the relevant interaction mode. Such wave functions are particularly useful when one is dealing with a situation in which a configuration interaction treatment is needed. Because the same basis states are used in the construction of all the many-body wave functions, it is possible to easily calculate overlaps and interaction matrix elements for the many-body wave functions obtained from different values of the generator coordinates (which are not in general orthogonal). The valence space can contain a very large number of single-particle basis states, when there are constants of motion that can be used to break the levels up into sub-groups. To increase this size, we have parallelized our code to run on the SP computer system, and we are modifying the code to deal with octupole correlations in heavy nuclei.

Recently, our major effort was to extend our many-body code to include neutron-proton pairing interactions, in both the T = 0 and T = 1 modes. This involved putting neutrons and protons in the same subgroup. In dealing with blocked levels, in the case of a simultaneous treatment of T = 1 and T = 0 interactions, the variational amplitudes are complex. We extended the code to deal with these complex amplitudes.

c.6. Neutron-Proton Pairing (R. R. Chasman)

We extended[1] our many-body method to include n-p pairing, with full projection of neutron and proton particle number before doing a variational calculation. We also found that there is a new quantum number that holds exactly for collective states; *i.e.* those states in which no levels are blocked. This new quantum number (Q) is the number parity of the T = 0 and T = 1 n-p pairs. Fixing the number parity of one n-p mode fixes the other, when the number of neutrons and protons is fixed. This number parity is closely related to the isospin quantum number. The collective states are the ground states for N = Z nuclides. We project Q - before doing a variational calculation. By doing calculations that conserve Q, we find a remarkable multiplicity of degenerate levels in odd-odd nuclides, with N = Z (2m). Such multiplets are at or near ground for m = 1 or 2. The form of our variational wave function includes an explicit amplitude for 'alpha like' correlations in each level as well as the usual amplitudes for n-n, p-p and n-p pairs.

In odd-odd N = Z nuclei,[2] the ground state is a doublet, consisting of a Q = 0 and Q = 1 state, when the T = 0 and T = 1 pairing strengths are equal. The splitting of this ground state doublet affords some information about the relative strengths of the T = 0 and T = 1 pairing strengths. In Fig. V-15b we plotted the splitting of these two states as a function of the T = 0 pairing strength, while keeping the T = 1 pairing strength fixed. Results are displayed for two choices of energy level spacing, 1) equally spaced levels, and 2) a level system in which the five levels closest to the Fermi level are bunched together. Because the pairing correlations are stronger in the bunched level system, the splittings are larger.

[1] R. R. Chasman, Phys. Lett. B **524**, 81 (2002).
[2] R. R. Chasman, Phys. Lett. B **553**, 204 (2003).
[3] D. G. Jenkins *et al*., Phys. Rev. C **65**, 064307 (2002).

In addition to the collective states discussed above, there are configurations in which one or more levels are blocked. These configurations constitute the ground states of all odd-mass nuclides and are likely to be the ground state or close in energy to the ground state of odd-odd nuclei with increasing neutron excess. For these blocked levels, the amplitudes are complex. We extended our treatment of n-p pairing to include configurations with blocked levels. In Fig. V-15a, we display the level spectra in the two model odd-odd systems used in the splitting calculation discussed above. The notable feature here is the remarkable increase in level density near the ground state with increasing neutron number. This feature was noted[3] in an analysis of levels of odd-odd nuclei.

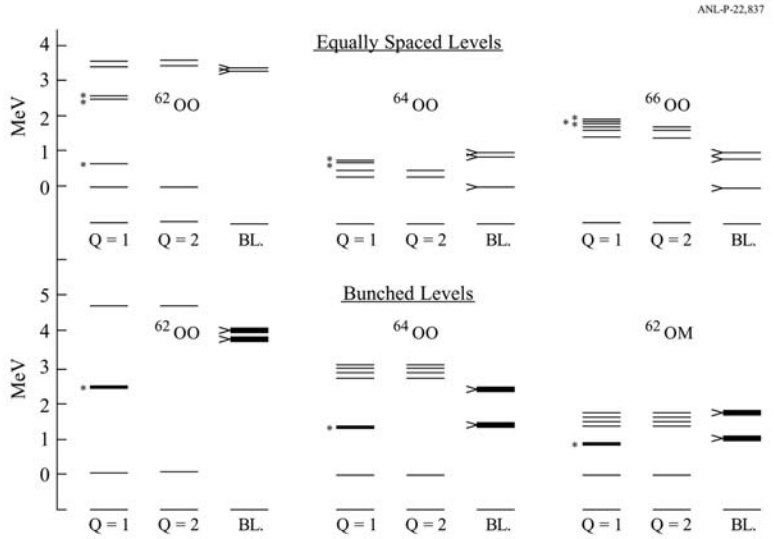

Fig. V-15a. Low-lying states in odd-odd nuclei near N = Z. BL (blocked) indicates configurations in which two levels have odd number parity and for which Q is no longer a good quantum number. The thick lines in the BL column in the bunched level scheme indicate a degeneracy of ten. The arrowhead on the left of all blocked levels indicates an additional factor of two in the number of levels coming from the two values of Ω with $\Omega = \Omega_1 \pm \Omega_2$. The Ω-blocked levels in the Q = 1 column are marked with an asterisk. The thick lines with asterisks in the bunched levels for Q = 1 have a degeneracy of five.

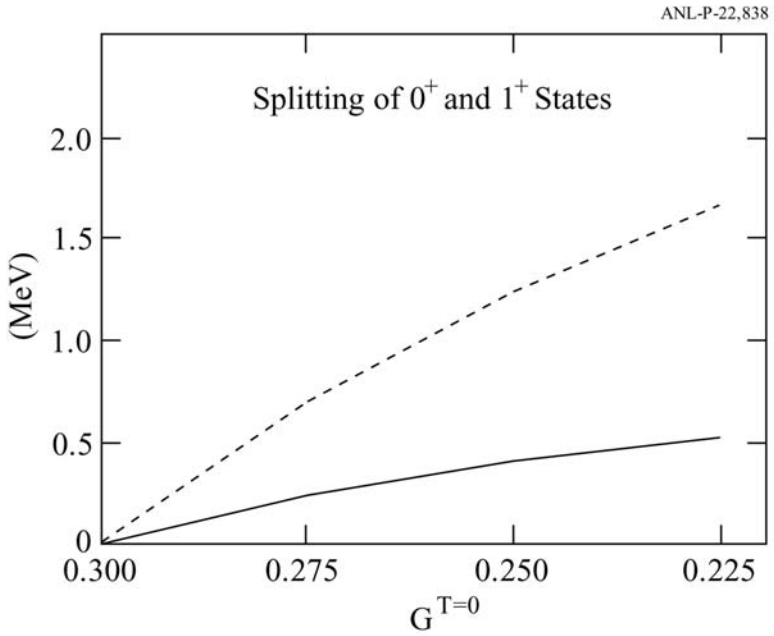

Fig. V-15b. Excitation energy of Q = 2 state in ^{62}OO as a function of $G^{T=0}$. $G^{T=1}$ has the value of 0.3 MeV. The dashed line gives the splitting for the bunched levels and the solid line is used for the equally spaced levels.

c.7. Octupole Correlations in Light Actinides (R. R. Chasman)

The difficulty in dealing with octupole correlations in the light actinides is that the effects are not sufficiently large to give rise to a well defined deformation. A many-body wave function is needed to deal effectively with these correlations. We started to apply our many-body approach to a re-examination of this region. In our early work, which was the first to predict parity doublets in the odd-mass nuclides of this region, we were limited to subgroups of at most five Nilsson orbitals. Advances in our code, and the use of parallel processing, make it feasible to deal with subgroups consisting of as many as eight Nilsson orbitals. One application of this calculation will be a study of the structure of the $½^{\pm}$ parity doublet in ^{225}Ra, that is being studied to put new upper limits on the dipole moment of the neutron.

c.8. Studies of Nuclear Energy Surfaces (R. R. Chasman, J. L. Egido,* and L. M. Robledo*)

This collaborative research program[1,2,3] focuses on the study of nuclear energy surfaces, with an emphasis on very deformed shapes using several complementary methods: 1) the Strutinsky method, 2) Hartree-Fock-Bogoliubov (HFB) calculations using the Gogny interaction, and 3) Many-Body (MB) variational wave functions that we described above. Our strategy is to identify phenomena and nuclides of interest using the Strutinsky method and to study the most interesting cases with the HFB and many-body (MB) approaches. The two latter approaches include many-body effects and describe these features more accurately.

The great advantage of the Strutinsky method is that one can study the energy surfaces of many nuclides (~300) with a single set of calculations. Although the HFB and MB calculations are quite time consuming relative to the Strutinsky calculations, they have many advantages. For the studies of Pb, they have the advantage that configuration interaction effects can easily be incorporated in the calculations. In this way, we deal directly with the issue of ensuring the orthogonality of states that have the same spins and parities. We recently examined the effects of angular momentum projection on the low-lying spectra of the even Pb isotopes in the HFB calculations. We find that angular momentum projection does not substantially bring down the energy of the oblate 0^+ state.

*Universidad Autonoma de Madrid.

[1]R. R. Chasman and L. M. Robledo, Phys. Lett. **B351**, 18 (1995).
[2]J. L. Egido, L. M. Robledo, and R. R. Chasman, Phys. Lett. **B393**, 13 (1997).
[3]R. R. Chasman, J. L. Egido, and L. M. Robledo, Phys. Lett. **B513**, 513 (2001).

c.9. Order Generated by Random Many-Body Dynamics (A. Volya and V. Zelevinsky)

We demonstrate a coexistence of quantum chaos and order in strongly interacting mesoscopic systems. In this study[1,2] we consider a simple shell-model system of one single-particle *j*-level that can host 2j + 1 identical fermions. The system is driven by random two-body interactions that preserve rotational symmetry. It was shown previously that the ground state spin has an unexpectedly large probability to be $J_0 = 0$.[3] The statistical model[4] predicts the probabilities of $J_0 = 0$ and $J = J_{max}$ (maximum spin possible) to be significantly enhanced. For the maximum spin this probability, however, is suppressed by the fact that the corresponding state is unique and does not obey statistical regularities. Now we consider excited states of random realizations with $J_0 = 0$ that dominate the statistics. We first chose those 5 to 15% of realizations where the ground state has $J_0 = 0$ while the first excited state has $J_1 = 2$. For these realizations we compare the values of the quadrupole moment of the $J_1 = 2$ state and the quadrupole transition strength, B(E2), from this state to the ground state. The resulting normalized histogram for the ratio $Q^2/B(E2)$ is shown in Fig. V-16. The dashed line indicates the value of this ratio for the rigid rotor. It is clear from the figure that selected systems, governed by interactions of random nature, exhibit collective properties of regular deformation.

This work shows collective features emerging in a finite many-body system with random dynamics. To trace the origin of this collectivity, one has to go beyond the

standard statistical descriptions and include non-linear correlations that shape the many-body mean field. The observed empirical results that come along with random interactions but exhibit generic collective features suggest that the robust realistic properties are not necessarily a result of a unique nature-chosen interaction, but rather a manifestation of kinematic rules and symmetries of a quantum mesoscopic system.

*Michigan State University.

[1]A. Volya and V. Zelevinsky, Proc. of the Wigner Centennial Conf., Pécs, Hungary (2002), pp. 10.
[2]V. Zelevinsky and A. Volya, Proc. of the 7th International Spring Seminar on Nuclear Physics, ed. A. Covello (World Scientific, Singapore, 2002) p. 261.
[3]C. W. Johnson, G. F. Bertsch, and D. J. Dean, Phys. Rev. Lett. **80**, 2749 (1998).
[4]D. Mulhall, A. Volya and V. Zelevinsky, Phys. Rev. Lett. **85**, 4016 (2000).

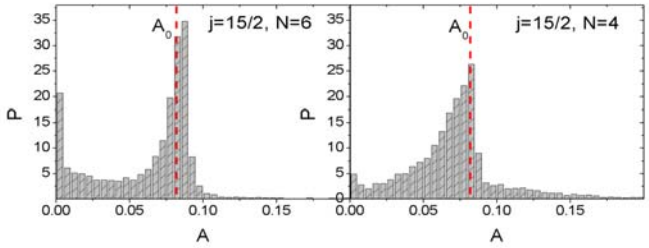

Fig. V-16. The normalized histograms display the distribution of the ratio $A = Q^2/B(E2)$ for all random realizations with $J_0 = 0$ and $J_1 = 2$, for the systems of $N = 4$ and $N = 6$ particles on a $j = 15/2$ orbital. The vertical dashed lines show the Alaga prediction for a rigid rotor.

c.10. Non-Hermitian Effective Hamiltonian and Continuum Shell Model

(A. Volya and V. Zelevinsky*)

The intrinsic dynamics of a system with open decay channels is described by a non-Hermitian and energy-dependent effective Hamiltonian. We discuss ways of incorporating this approach into the shell model context. Although the main ideas of the approach are well known, right now, with the main interests of nuclear studies shifted away from the line of stability, it seems to be an appropriate moment to revive them and convert into a working tool for the solution of numerous practical problems of nuclear theory. The applications of the approach are not limited to nuclear physics; they were found useful in optics, see Ref. 1 and references therein, in atomic physics, condensed matter, physics of microwave cavities, theory of measurement and quantum computing.

We view the effective Hamiltonian as a sum of three terms,

$$\mathcal{H} = \mathrm{H}^{\circ} + \mathrm{V} - \frac{\mathrm{i}}{2}\mathrm{W(E)}, \qquad (1)$$

where the intrinsic Hermitian part $H^o + V$ consists of independent particle energies, and the effective Hermitian interaction V is assumed to include renormalization terms generated by the virtual coupling through continuum. The imaginary part W(E) originates from the real processes of decay to channels that are open at a given energy. It is represented by the residues of the on-shell terms corresponding to the delta-functions coming from the energy conservation and causality requirements imposed on the energy denominators.

At this stage,[2] a phenomenological form of the effective Hamiltonian borrowed from a traditional shell model is extended with new energy-dependent non-Hermitian terms that are parameterized in a way properly representing the kinematics of reaction processes near thresholds. The main goal here is to develop and discuss methods for solving the many-body problem with the use of the effective Hamiltonian (1). Besides the fact that internal dynamics are represented by a non-

Hermitian Hamiltonian responsible for decays, the calculations require a correct account of threshold singularities in the amplitudes of the processes at low energies. We also emphasize the need for self-consistency of two types, (i) regular solution for the complex energies of quasistationary states governed by the energy-dependent Hamiltonian and (ii) the consistent determination of bound state energies, open channels and reaction thresholds for a chain of nuclides connected by those channels. The latter implies that the new continuum shell model, in contrast to its traditional analog, treats the whole range of nuclei, linked by reactions, in a single picture with a common effective interaction. Such a continuum treatment almost certainly requires new computational efforts and the method we employed, an hybrid of the exact solution for the pairing interaction with the interaction through the continuum seems to be a promising instrument for future development.

Table V-I. Seniority s = 0 and s = 1 states in oxygen isotopes. Energies and neutron decay widths are shown. Results are compared to the full shell model calculations and to known experimental data. Ground state energies relative to the ^{16}O core are given in bold. The rest of the energies are excitation energies in a given nucleus.

A	J	E	Γ	$E_{s.m.}$	$E_{exp.}$	$Γ_{exp.}$
		(MeV)	(keV)	(MeV)	(MeV)	(keV)
16	0	**0.00**	0	**0.00**	**0.00**	0
17	5/2	**-3.95**	0	**-3.95**	**-4.14**	0
17	1/2	0.78	0	0.78	0.87	0
17	3/2	5.59	96	5.59	5.08	96
18	0	**-12.17**	0	**-12.17**	**-12.19**	0
19	5/2	**-15.75**	0	**-16.06**	**-16.14**	0
19	1/2	1.33	0	1.47	1.47	0
19	3/2	5.22	101	5.53	6.12	0
20	0	**-23.41**	0	**-23.83**	**-23.75**	0
21	5/2	**-26.67**	0	**-27.47**	**-27.55**	0
21	1/2	1.38	0	1.33		
21	3/2	4.60	63	4.83		
22	3/2	**-33.94**	0	**-34.62**	**-34.40**	0
23	1/2	**-35.78**	0	**-37.07**	**-37.15**	0
23	5/2	2.12	0	2.72		
23	3/2	2.57	13	3.28		
24	0	**-40.54**	0	**-41.05**	**-40.85**	0
25	3/2	**-39.82**	14	**-40.28**		
25	1/2	2.37	0	2.36		
25	5/2	4.98	0	3.96		
26	0	**-42.04**	0	**-42.04**		
27	3/2	**-40.29**	339	**-40.29**		
27	1/2	3.42	59	3.42		
27	5/2	6.45	223	6.45		
28	0	**-41.26**	121	**-41.26**		

As one demonstration of the techniques developed, we present a realistic self-consistent shell model calculation for oxygen isotopes in the mass region A = 16 to 28, TableV-I. In this study we use a universal *sd*-shell model description with the semi-empirical effective interaction, restricted to pairing and monopole components. Despite these simplifications, the overall agreement with the observed data is good. In our view, however, the main merit of this calculation is in demonstrating the power of the method.

*Michigan State University.

[1]A. Volya and V. Zelevinsky, Tech. Rep., ANL (2002); LANL preprint quant-ph/0303010.
[2]A. Volya and V. Zelevinsky, ANL preprint PHY-10327-TH-2002; LANL preprint nucl.th/0211039.

c.11. Two-Dimensional Calculations of Nuclei in a Chiral Model (S. Schramm)

From the point of view of nuclear structure there has been significant progress in describing finite nuclei using relativistic meson field models. Those calculations are quite successful in describing nuclear properties over a wide range of mass numbers.

It is possible to obtain sensible behavior of excited matter, a good description of nuclear saturation as well as of nuclei and hypernuclei with a single model and a single set of parameters. I based the investigation on a hadronic model with chirally symmetric interactions incorporating flavor-SU(3) symmetry to calculate nuclear properties within this approach. I determined a new improved set of model parameters generated by a fit to properties of a set of spherical nuclei. The results showed that the quality of the description of nuclear properties is about at the same level of accuracy and even slightly exceeds the one of the currently used most successful dedicated relativistic nuclear structure approaches. For the first time in this context the isospin-triplet meson was taken into account, which naturally occurs within the SU(3) scheme in its coupling to the baryons as well as in the nonlinear meson-meson interactions.

I investigated deformed nuclei in a 2-dimensional nuclear calculation and found good results for nuclear quadrupole deformations in comparison with available data. A study of possible superheavy elements did not show any distinct magic numbers for neutrons as well as for proton numbers that could be deduced from the gap energies as shown in Fig. V-17. Currently I am extending the investigation by considering a number of improvements. This includes a projection onto good particle numbers as well as, in case of the deformed calculations, a projection onto good angular momentum. Also first three-dimensional studies were performed and a calculation including configuration mixing is underway.

[1]S. Schramm, Phys. Rev. C **66**, 064310 (2002).

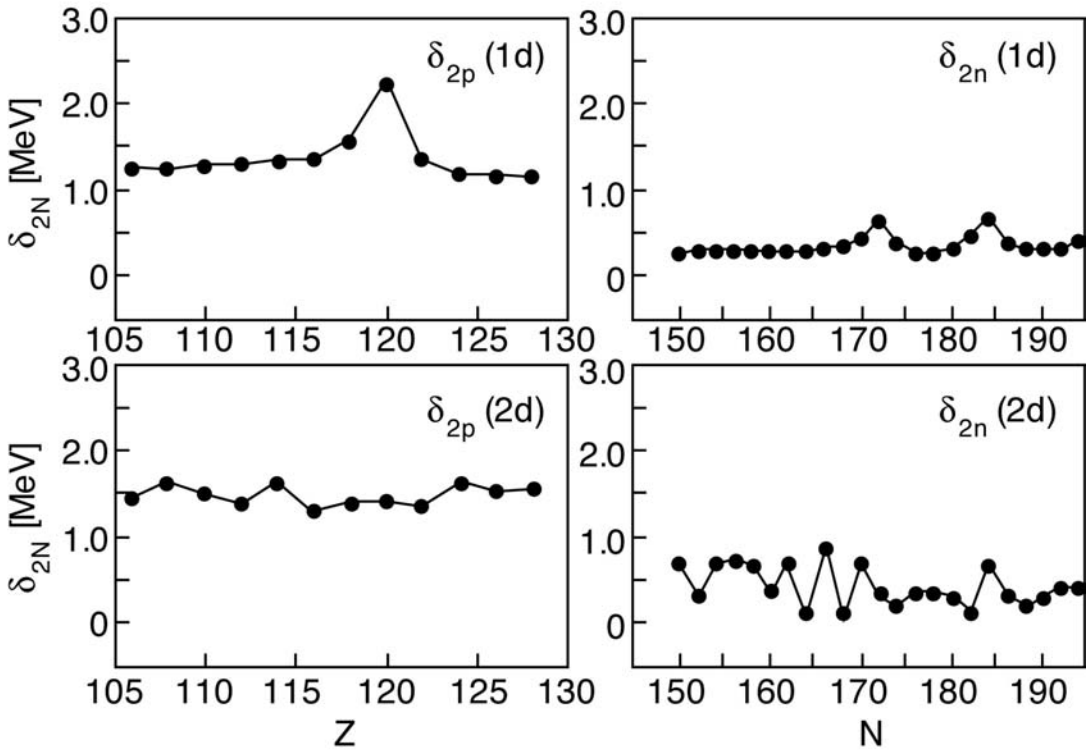

Fig.V-17. The figure shows the two-nucleon gaps δ_{2p} (left panels) and δ_{2n} (right panels) in units of MeV. Results for superheavy nuclei are shown. The upper panels show the results of a calculation assuming spherical symmetry. The lower panels display the results from a 2-dimensional calculation assuming axial symmetry.[1]

c.12. Rotating Neutron and Hyperstars (S. Schramm and D. Zschiesche*)

Neutron star properties can give important clues for understanding the isospin dependence of nuclear forces. The most directly observable property of a neutron star is its rotational frequency, through its pulsar radio signals emitted from the magnetic poles of the star. It is crucial to relate star properties with other isospin-sensitive observables like neutron distribution radii in neutron-rich nuclei or multi-fragmentation in heavy-ion collisions with different N/Z nuclei.

This is the motivation for developing and applying a hadronic model with a broad applicability including the regime of infinite nuclear matter, finite nuclei and chiral symmetry restoration to relate predictions in the various areas. As at high densities it is favorable to populate hyperonic states in addition to nucleons inside of the star, the model is based on SU(3) in flavor space.

We extended our calculations of static neutron stars and hyperstars to study the properties of rotating neutron (hyper-) stars. To this end we extend the theoretical treatment of static systems based on the solution of the Tolman- Oppenheimer-Volkov equations for the star structure by following the formalism developed by Hartle and Thorne to treat the general relativistic equations for the structure of rotating stars. In order to solve those equations we first determined the equation of state and its hyperonic matter contributions, and then integrated the differential equations for the metric tensor inside of the star, which determines its structure and shape.

As shown in Fig. V-18 the resulting star shapes show a significant eccentricity for rapidly rotating stars (comparable to that of superdeformed nuclei), which also effects a deformation of its hypermatter distribution in the interior of the star. The moment of inertia shows a strong dependence on the rotational frequency. This needs to be taken into account for determining the spinning-down behavior of the pulsar.

We did not find a back-bending of the inertia with decreasing rotational frequency as was suggested by other authors. For such a back-bending effect to occur, the interior of the star has to go through major structural changes during the spin-down as is the case for the

analogous phenomenon in rapidly rotating nuclei due to pairing breakup. In the present calculation the slow transition of the hadronic model towards chiral restoration at high densities and low temperatures prohibits any major observable effects. However, we found possible transitions of rapidly rotating pure neutron stars that convert to hyperstars during the slowdown of the pulsar.

The calculations showed that, owing to rotation, the maximum star mass can be increased from 1.64 to 1.94 solar masses compared to the case of a static star.[1] This value still shows a clear reduction from projections of star calculations without hyperons which typically show mass limits beyond 2 solar masses. With more observational data being collected it would be interesting to see whether a relation between masses and pulsar frequencies can be established.

With regard to maximum star masses a discussion of the possible effects of populating higher baryonic resonances in the neutron star should be performed. Those additional degrees of freedom might change the high-density behavior of the system significantly, generating a different structure of the time-evolution of the rotating star. Such a calculation might set tight constraints on the theoretical descriptions of hadronic resonances and their couplings to other fields by studying their effect on neutron star properties, especially on the star's mass. We are currently investigating this point.

*University of Frankfurt.

[1]S. Schramm and D. Zschiesche, J. Phys. G: Nucl. Part. Phys. **29**, 531 (2003).

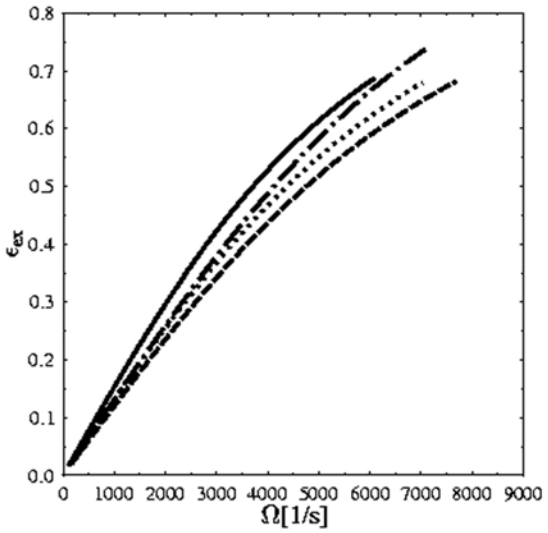

Fig. V-18. The figure shows the eccentricity of the deformed rotating neutron star as function of rotational frequency $\Omega = 2\pi\nu$ for different masses for the static neutron star.[1]

c.13. The Effective Interaction in Nuclei for Calculations Beyond the Mean-Field

(T. Duguet, M. Bender,* H. Heenen,* P. Bonche,† and J. Meyer‡)

We extended the standard Goldstone-Brueckner perturbation theory to motivate methods beyond the mean-field, such as the Generator Coordinate Method or the Projected Mean-field Method, from a perturbative point of view for the first time. We derived the effective interaction removing the hard-core of the bare nucleon-nucleon force accordingly. Simplifying this effective vertex, we proposed an extended version for the Skyrme interaction, which is valid for configuration mixing calculations.

We started to perform calculations beyond the mean-field level to validate this extended Skyrme model quantitatively. Here, it is interesting to concentrate on exotic properties of nuclei, where correlations associated with the restoration of symmetries broken at the mean-field level and large amplitude vibrations are crucial to reproduce the data. As a first topic, we are studying shape coexistence in neutron-deficient lead, mercury and polonium isotopes by configuration mixing of symmetry-restored HFB wave functions. The main issue is to understand the interplay of the

interaction properties to describe shape isomerism correctly in the whole mass region. In particular, we intend to illustrate the importance of the density dependence of the interaction. At the same time, we will learn about other properties of the interaction such as its surface tension, its pairing channel, and the single-particle spectra it generates. Indeed, the quantitative description of shape isomerism results from the delicate combination of all these characteristics. To go one step further, we need to probe the effective interaction in different mass regions and for different nuclear properties. To do so, we started calculations beyond the mean-field to study shape isomerism in tin isotopes and shell quenching towards the drip-lines in lighter nuclei.

*Universite Libre de Bruxelles, Belgium, †CEA/Saclay, France, ‡IPNL/CNRS-IN2P3, France.

c.14. Probing the Gateway to Superheavy Nuclei in Cranked Relativistic Hartree-Bogoliubov Theory (A. V. Afanasjev, T. L. Khoo, I. Ahmad, S. Frauendorf,* and G. A. Lalazissis†)

The cranked relativistic Hartree-Bogoliubov theory (CRHB), including approximate particle number projection through the Lipkin-Nogami method and the Gogny force in the particle-particle pairing channel, was employed in a systematic study of the nuclei around ^{254}No. The deformation, rotational response, pair correlations, quasiparticle spectra, nucleon separation energies and shell structure of these nuclei were extensively studied with different RMF forces.

While the deformation properties are well reproduced, the calculations reveal that an accurate description of other observables requires better model forces both in the particle-hole and particle-particle channels. The calculated moments of inertia show only small sensitivity to the RMF force and thus to the details of the single-particle structure. In contrast to previous studies, where the moments of inertia in lighter systems are well reproduced, good agreement in the heaviest nuclei can only be obtained with a decrease (≈ 12%) of the strength of the D1S Gogny force in the pairing channel.

The CRHB theory was extended for a detailed description of quasi-particle states in odd and odd-odd nuclei. For the first time, the blocking procedure in such nuclei was performed fully self-consistently, with effects of the breaking of time-reversal symmetry (nuclear magnetism) taken into account. Analysis of quasi-particle spectra in odd ^{249,251}Cf and ^{249}Bk nuclei with the NL1 and NL3 forces suggests that the energies of most spherical orbitals, from which active deformed states of these nuclei emerge, are described with an accuracy of better than 0.5 MeV. However, for a few subshells the discrepancies reach 1.0 MeV. As the RMF forces were only fitted to bulk properties of spherical nuclei without considering single-particle energies, this level of agreement is impressive. However, in very heavy systems, where the level density is high, the accuracy is not sufficient for reliable predictions of the location of deformed shell gaps, which are small (≈1 MeV).

The results of our analysis have implications for the study of superheavy nuclei. The NL-SH and NL-RA1 forces do not provide satisfactory descriptions of the single-particle energies: the deviations between experiment and theory in the $A \sim 250$ mass region reach 2 MeV for some spherical subshells. Hence their application to superheavy nuclei is not recommended. The extrapolation of the results for quasiparticle states obtained in the $A \sim 250$ mass region suggests that the NL1, NL3 and NL-Z forces provide reasonable descriptions of most of the states in the vicinity of the $Z = 120$ and $N = 172$ spherical shell gaps. However, it is not possible to estimate the accuracy of the description of some low-j states, such as $\nu 3d_{3/2}$, $\nu 4s_{3/2}$ and $\pi 3p_{3/2}$, $\pi 3p_{1/2}$, which are located near these gaps. Thus the particle numbers corresponding to magic gaps in superheavy nuclei remains an open question. An article describing this research was published.[1]

*University of Notre Dame, †Aristotle University, Thessaloniki, Greece.

[1]A.V. Afanasjev et al., Phys. Rev. C 67, 024309 (2003)

D. ATOMIC THEORY AND FUNDAMENTAL QUANTUM MECHANICS

In addition to research on hadronic and nuclear physics, we also conduct research in atomic physics, neutron physics, and quantum computing.

Work in atomic physics includes the studies of interactions of electrons or high-energy photons with matter, in support of experiments performed at Argonne's Advanced Photon Source (APS). Theoretical studies are being conducted on the physics of the photoeffect and Compton scattering by bound electrons, focusing on topics selected in view of basic importance, timeliness, and potential in applications. Data on crystalline silicon for the interactions of photons over the entire spectral range were comprehensively analyzed with the use of dispersion relations and sum rules, and results are being prepared for publication. Cross sections for triple ionization of atomic lithium by electron impact, measured by Argonne colleagues, were theoretically interpreted.

Theoretical work in support of a new experiment to measure the neutron electric-dipole moment continues. The principal current focus is on a preliminary proof-of-principle experiment to measure the neutron magnetic-dipole moment in the same way. In addition, an analysis of the basis of the spin-statistics theorem in nonrelativistic quantum mechanics has shown that spin-zero particles must obey boson statistics without the assumptions of quantum field theory. Continuing work seeks to discover what additional assumptions are needed to extend that result to non-zero spins.

Work in areas related to quantum computing continued by completing an investigation of cyclic networks of quantum gates. The work was the research component of a Ph. D. thesis given by the University of Michigan to a graduate student working at Argonne.

In addition, work was completed on a framework for developing a coherent theory of mathematics and physics together. This research was partly based on the universal applicability of quantum mechanics, and the requirements that: such a theory be maximally valid and strong, and describe its own validity and strength to the maximum extent possible. This work and other studies of the necessary physical nature of language were the bases for initiating research on resource limited theories and their extensions as an approach to a theory of everything. The ideas developed are based on a well known but unappreciated relation between the size of the physical system investigated, the indirectness of the reality status of system properties being investigated, and physical resources needed for the investigations.

d.1. Interactions of Photons with Matter (M. Inokuti and D. Y. Smith*)

In support of experiments in atomic and condensed-matter physics with the use of synchrotron radiation, theoretical studies are being conducted on the physics of photo-absorption and Compton scattering, focusing on topics selected in view of basic importance, timeliness, and potential applications.

One theme of long-term studies has been the use of dispersion relations and sum rules for indices of response of matter over the entire range of photon energies. A comprehensive analysis of optical data on silicon is nearly complete, and is being prepared for publication. A novel method for characterizing the refractive index of a substance in a region of near transparency was formulated and applied to silicate glasses.[1]

*University of Vermont.

[1]D. Y. Smith, M. Inokuti, and W. Karstens, Radiat. Effects Defects Solids **157**, 823 (2002).

d.2. Interactions of Charged Particles with Matter (M. Inokuti)

Stopping power, the total yield of ionization, and its statistical fluctuations are examples of quantities describing the penetration of charged particles through matter and are important to applications such as the detection of particles and the analysis of their charges and kinetic energies. The understanding of those quantities in terms of individual collisions and associated cross sections remains a major challenge and is the goal of our continuing effort.

For instance, the cross section for triple ionization of the lithium atom by electron impact, recently measured by Argonne colleagues, was interpreted.[1]

An essay[2] on the role of physics in radiation sciences was written in commemoration of the 50th Anniversary of the Radiation Research Society. Extensive work for the International Commission on Radiation Units and Measurements (ICRU) continues on the editing of its reports and on physical data such as stopping powers and various interaction cross sections.

[1]M.-T. Huang, W. W. Wong, M. Inokuti, S. H. Southworth, and L. Young, Phys. Rev. Lett., in press.
[2]M. Inokuti and S. M. Seltzer, Radiat. Res. **158**, 3 (2002).

d.3. Spin and Statistics in Nonrelativistic Quantum Mechanics: The Spin-Zero Case (Murray Peshkin)

I completed a proof from stated assumptions of ordinary nonrelativistic quantum mechanics based on the Schrödinger equation that identical spinless particles with no degrees of freedom other than the spatial ones must obey symmetric statistics. The key assumption is one introduced earlier by Leinaas and Myrheim, that the configuration space for two particles must consist of the unordered pairs $\{\mathbf{r}_1,\mathbf{r}_2\}$. That assumption is the mathematical implementation of the physical principle that the dynamical variables in the theory should be in one-to-one relation with the physically measurable quantities. Then the indistinguishability of the two particles is reflected by the wave function for spin-zero particles depending upon the unordered pairs, for which $\{\mathbf{r}_2,\mathbf{r}_1\}=\{\mathbf{r}_1,\mathbf{r}_2\}$. Leinaas and Myrheim were able to show that this assumption and its generalization to non-zero spins limit the possible statistics to fully symmetric or fully antisymmetric, eliminating intermediate statistics. Berry and Robbins later extended the work of Leinaas and Myrheim, giving a precise mathematical treatment of the problem for all spins and relating the statistics to the topology of the configuration space, but they too were unable to eliminate the "wrong" statistics for any spin. I was able to eliminate antisymmetric statistics for identical spin-zero particles by using an additional assumption, that the wave functions must be continuous because of the second derivatives in the Hamiltonian. Ongoing research seeks to relate these considerations to the proofs from quantum field theory, which appear superficially to have an entirely different physical basis. I am also attempting to generalize the nonrelativistic proof to include nonzero spins.

d.4. The Representation of Numbers in Quantum Mechanics (P. Benioff)

Work on quantum mechanical representations of natural numbers, integers, and rational numbers was published.[1] The representations were based on the use of creation and annihilation operators for bosons and fermions to represent numbers in a k-ary basis as states of quantum systems. Products of the same operators were used to represent various arithmetic operations on the states representing numbers. The importance of the requirement of efficient implementability for physical models of the axioms was emphasized. This condition requires the use of successor operations for each value of j, corresponding to addition of k^{j-1} if $j > 0$ and (for rational numbers) k^j if $j < 0$. It follows from the efficient implementability of these successors, which are used in all computers, that implementation of the addition and multiplication operators, which are defined in terms of iterations of the successors, should be efficient. Implementation of definitions of the addition and multiplication operators based on the successor for $j = 1$ only, which is the only successor defined in the usual axioms of arithmetic, are not efficient.

[1]P. Benioff, Algorithmica. **34**, 529-559 (2002).

d.5. Towards a Coherent Theory of Mathematics and Physics (P. Benioff)

Work was completed on a description of a framework for developing a coherent theory of mathematics and physics together.[1] The two main requirements that such a theory must satisfy are that it is valid and sufficiently strong, and it must maximally describe its own validity and sufficient strength. The mathematical logical definition of validity is used. This says that a theory is valid if all theorems of the theory are true in any domain of the theory. Other aspects of a coherent theory include universal applicability, the relation to the anthropic principle, and possible uniqueness. The requirement that the coherent theory maximally describe its own validity and completeness follows from universal applicability in that intelligent systems, and experimental and computational equipment are all included in the domain of the theory. It follows that the dynamical process of validation of the theory is in the theory domain, so the theory must describe in some sense its own validation. The uniqueness possibility would hold if the two basic requirements were so restrictive that only one theory can satisfy them. The work suggests that the basic properties of the physical and mathematical universes are entwined with and emerge with a coherent theory. Support for this includes the indirect reality status of properties of very small or very large far away systems compared to moderate sized nearby systems. Discussion of the necessary physical nature of language includes physical models of language and a proof that the meaning content of expressions of any axiomatizable theory seems to be independent of the algorithmic complexity of the theory. Gödel maps seem to be less useful for a coherent theory than for purely mathematical theories because all symbols and words of any language must have representations as states of physical systems. These states are already in the domain of a coherent theory.

[1]P. Benioff, Foundations of Physics, **32**, 989-1029, (2002).

d.6. Language is Physical (P. Benioff)

Work was completed on some aspects of the physical nature of language.[1] In particular, physical models of language must exist that are efficiently implementable. The existence requirement is essential because without physical models no communication or thinking would be possible. Efficient implementability for creating and reading language expressions is discussed and illustrated with a quantum mechanical model. Physical states of systems that represent language expressions can have meaning, either as an informal language or as a formal language associated with mathematical or physical theories. Any universally applicable physical theory, or coherent theory of physics and mathematics together, includes in its domain physical models of expressions for both the informal language used to discuss the theory and the expressions of the theory itself. It follows that some formulas in the formal theory express some of their own physical properties.

[1]Prepared from notes for talk at 1st Feynman Festival, Univ. Maryland, Aug., 2002 (to appear in Quantum Information Processing).

The inclusion of intelligent systems in the domain of the theory means that the theory, *e.g.* quantum mechanics, must describe, in some sense, its own validation. Maps of language expressions into physical states are discussed. A spin projection example is considered, as are conditions under which such a map is a Gödel map.

d.7. Resource-Limited Theories and their Extensions: A Possible Approach to a Theory of Everything (P. Benioff)

Work was begun on resource-limited theories and their extensions as a possible approach to a coherent theory of physics and mathematics or, for short, a theory of everything. The work, which is based on earlier research,[1] starts with the idea that the extension of physical and mathematical theories to include the amount of space, time, momentum, and energy resources required to determine properties of systems may influence what is true in physics and mathematics at a foundational level. One proceeds by associating to each amount, r, of resources a domain, D_r, a theory, T_r, and a language, L_r. D_r is limited in that all statements in D_r require at most r resources to verify or refute. T_r is limited in that any theorem of T_r must be provable using at most r resources. Also any theorem of T_r must be true in D_r. L_r is limited in that all expressions in L_r require at most r resources to create, display, and maintain. Consequences of these resource limitations are being investigated with a goal of further characterizing the theories and describing the use of resources by observers to develop theories of physics and mathematics.

[1] P. Benioff, Foundations of Physics **32**, 989-1029, (2002); Quantum Information Processing, (quant-ph 0210211).

d.8. Cyclic Networks of Quantum Gates (Paul Benioff and Peter Cabauy*)

Work was completed on initial steps in an analysis of cyclic networks of quantum gates. These networks include feedback loops as well as external lines. All one and two qubit networks with one and two loops were investigated as well as two qubit networks with a third qubit on an external line. The analysis included a group theory classification of the networks, a study of their dynamics, and perturbation effects induced by the third, external qubit. Some ideas on the use of cyclic networks in quantum algorithms, quantum memories, and quantum sensors were discussed. This work provided the bulk of a Ph. D. Thesis awarded to Peter Cabauy from the University of Michigan in the fall of 2002. A paper was submitted to Physical Review A.

*ANL and University of Michigan.

E. OTHER ACTIVITIES

e.1. Hadron Structure and GeV Electroweak Interactions (T.-S. H. Lee)

In the past few years, a large amount of high precision data on the nucleon's electromagnetic reactions in the few-GeV energy region was accumulated in experiments at several laboratories around the world. Furthermore, there is a possibility that high quality neutrino scattering data in the same energy region could soon become available at Fermi Laboratory and also at several neutrino facilities currently under construction. These developments provide tremendous opportunities for understanding non-perturbative aspects of hadron structure. To aid in exploiting these opportunities, the Theory Group hosted a workshop in the week of July 29 – August 2, 2002, whose goal was to focus attention on the theoretical challenges that the data presents, and encourage and facilitate collaborative research. There were twenty invited talks on subjects ranging from nucleon structure and nucleon resonances, through simulations of lattice QCD and models of electroweak reactions; and there was also ample time for discussions between the forty participants drawn from around the world. Articles stimulated by discussions at the Workshop have begun to appear.

e.2. 15th Annual Midwest Theory Get-Together (C. D. Roberts)

The Theory Group hosted the fifteenth Annual Midwest Theory Get-Together on October 25-26, 2002. Nuclear theorists from eight Midwest universities, FNAL and ANL met to learn about the research goals and foci of different individuals and groups throughout the region. While the organizational duties rotate amongst the participants, Argonne is the regular host site because of its meeting facilities and central location. The organizers for 2002 were Timothy Londergan and Adam Szczepaniak of Indiana University in Bloomington. The meeting provides a good chance for students to broaden their outlook and get some practical speaking experience in a friendly atmosphere. The format is informal, with an agenda of talks being volunteered at the beginning of the meeting. In 2002 we had thirty-four registered participants: faculty, postdocs and students. Over the Friday afternoon and Saturday morning approximately twenty-five presentations were made, covering topics such as: relativistic heavy ion collisions; no-core shell model; nuclear pairing; nucleon matter; quantum Monte-Carlo methods; wavelet methods for few body physics; effective field theories; hadron physics; and QCD. No one left unhappy.